JOINT TRANSPORTATION
RESEARCH PROGRAM
INDIANA DEPARTMENT OF TRANSPORTATION
AND PURDUE UNIVERSITY

Guidelines for Use and Design of Deep Foundations for Three-Sided Structures

Yao Wang, Rodrigo Salgado, and Monica Prezzi

SPR-4732 • Report Number: FHWA/IN/JTRP-2026/07 • DOI: 10.5703/1288284318615

RECOMMENDED CITATION

Wang, Y., Salgado, R., & Prezzi, M. (2026). *Guidelines for use and design of deep foundations for three-sided structures* (Joint Transportation Research Program Publication No. FHWA/IN/JTRP-2026/07). West Lafayette, IN: Purdue University. https://doi.org/10.5703/1288284318615

AUTHORS

Yao Wang
Purdue University

Rodrigo Salgado, PhD, PE, JD
Purdue University
765-494-5030
rodrigo@purdue.edu
Corresponding Author

Monica Prezzi, PhD
Purdue University

ACKNOWLEDGMENTS

We are grateful to Jeremy Hunter and Peter White for identifying this research need. We are thankful for Peter White for the numerous conversations about design aspects of three-sided structures and for his insightful comments. We are also thankful to Timothy Wells's support and guidance throughout the project and for his perspectives on the function of three-sided structures in transportation projects. We also thank all members of the study advisory committee—Min Sang Lee, Joshua Heigert, and Jeremy Hunter—for their guidance throughout the project.

JOINT TRANSPORTATION RESEARCH PROGRAM

The Joint Transportation Research Program serves as a vehicle for INDOT collaboration with higher education institutions and industry in Indiana to facilitate innovation that results in continuous improvement in the planning, design, construction, operation, management and economic efficiency of the Indiana transportation infrastructure. Learn more at engineering.purdue.edu/JTRP.

Published reports of the Joint Transportation Research Program are available at docs.lib.purdue.edu/jtrp/.

NOTICE

The contents of this report reflect the views of the authors, who are responsible for the facts and the accuracy of the data presented herein. The contents do not necessarily reflect the official views and policies of the Indiana Department of Transportation or the Federal Highway Administration. The report does not constitute a standard, specification, or regulation.

TECHNICAL REPORT DOCUMENTATION PAGE

1. Report No.	2. Government Accession No.	3. Recipient's Catalog No.
FHWA/IN/JTRP-2026/07		

4. Title and Subtitle	5. Report Date
Guidelines for use and design of deep foundations for three-sided structures	February 11, 2026
	6. Performing Organization Code

7. Author(s)	8. Performing Organization Report No.
Yao Wang Rodrigo Salgado, PhD, PE, JD (https://orcid.org/0000-0002-8706-3279) Monica Prezzi, PhD (https://orcid.org/0000-0002-3598-5423)	FHWA/IN/JTRP-2026/07

9. Performing Organization Name and Address	10. Work Unit No.
Joint Transportation Research Program Hall for Discovery and Learning Research (DLR), Suite 204 207 S. Martin Jischke Drive West Lafayette, IN 47907	**11. Contract or Grant No.** SPR-4732

12. Sponsoring Agency Name and Address	13. Type of Report and Period Covered
Indiana Department of Transportation (SPR) State Office Building 100 North Senate Avenue Indianapolis, IN 46204	Final Report
	14. Sponsoring Agency Code

15. Supplementary Notes

Conducted in cooperation with the U.S. Department of Transportation, Federal Highway Administration.

16. Abstract

Buried three-sided structures are widely used for roadway crossings and underpasses. Whereas spread footings are common, deep foundations are required when weak soils, scour risk, or site constraints exist. This study aimed to improve understanding of load-transfer mechanisms and develop guidance for the design of deep foundations supporting buried three-sided structures.

A nationwide survey of 34 state DOT engineers and 12 three-dimensional finite element analyses were conducted. Results show that greater stem wall height and thicker earth cover lead to a more uniform live-load distribution between piles. The most critical condition occurs when the design truck is placed near the roadside, where piles beneath the loaded segment carry the greatest loads. When the truck is centered, the load distribution becomes nearly uniform, and the superposition principle approximately holds for well-designed to conservatively designed piles. Comparison with the traditional moment-of-inertia method indicates that the method overpredicts live loads by about 10%–50%. The study confirms that live-load moments are small enough to be neglected and that current design practice is conservative. These findings provide a rational basis for improved design guidance for pile-supported three-sided structures.

17. Key Words	18. Distribution Statement
three-sided structure, finite element analysis, live load distribution	No restrictions. This document is available through the National Technical Information Service, Springfield, VA 22161.

19. Security Classif. (of this report)	20. Security Classif. (of this page)	21. No. of Pages	22. Price
Unclassified	Unclassified	36	

EXECUTIVE SUMMARY

Buried three-sided structures are often used for roadway water crossings and pedestrian underpasses. While spread footings are commonly used, deep foundations become necessary when weak soils, scour potential, or site constraints are present. Design approaches for distributing loads to piles remain limited and rely heavily on engineering judgment. This research was undertaken to improve understanding of load transfer mechanisms and to develop guidance for deep foundation design supporting buried three-sided structures.

The study combined a nationwide survey of 34 state department of transportation (DOT) engineers with 12 three-dimensional (3D) finite element analyses (FEAs). The survey confirmed notable variability in how engineers estimate load distribution among piles, limited use of soil–structure interaction modeling, and common concerns regarding settlement, live load effects, and moment transfer at the stem wall–structure interface. The reference FEA model represented a typical buried three-sided structure with a 7.8 m (25.6 ft) span, 3.8 m (12.5 ft) height, and 12.1 m (39.7 ft) length supported on a pile cap. Realistic soil constitutive models were used, with frictionless contact between the structure and footing, perfect contact between the footing and soil, roller boundaries on the vertical sides of the model, and infinite elements at the bottom. In a parametric study, we analyzed the impact of varied soil profile, pile type (floating pile or tip bearing pile scenario), earth cover, segment width, shear key depth, stem wall height, truck position, and the number of trucks on live load transfer to the piles.

Under the modeled conditions and ranges investigated, earth cover and stem wall height influenced the load distribution across the piles. Increased stem wall height leads to a more uniformly distributed live load, which is preferable. Increased earth cover depth also reduces the magnitude of the maximum live load carried by the individual piles. Shear key depth does not have an impact on the live load distribution; instead, the shear key configuration has an impact on the moment transfer mechanism. However, under either scenario, the moments transferred to the individual piles are small enough to be considered negligible. The most critical scenario occurs when the truck is placed close to the roadside, where the piles beneath the loaded section can carry approximately 20% of the total live load transferred to the piles, while the piles that are furthest from the truck make almost no contribution. If the truck is placed at the center of the road, the live load distribution becomes more uniform, and all of the piles contribute comparably. Segment width does not have a significant impact on the live load distribution. A slightly over-consolidated clay layer on top of the clay layer surrounding the pile does not have a significant impact either.

The simulation results were compared with the traditional moment-of-inertia design method. The comparison shows that the traditional design method tends to overpredict the live load distributed to the piles, not only because it usually ignores the load absorbed by the backfill soil surrounding the structure and the footings, but also because the assumption adopted by the traditional method that the load will be distributed linearly among the piles in the pile group. Without considering the contribution of the soil and structures above the piles, the traditional method overpredicts the live load by 50%. Considering the contribution of the soil and the structures above the piles, the traditional method overpredicts the live load by 10–15%. With this level of overprediction, the traditional method could still be used to perform preliminary design. It should also be noted that the study evaluated only a 12 m (approximately 40 ft) long structure, and the conservatism associated with the method's underlying assumptions may decrease as structural length increases.

The findings apply to structure configurations, soil conditions, and loading conditions similar to the assumptions used in this study. Applicability of results should be evaluated on a project-specific basis, particularly for different soil profiles, geometric configurations, construction details, or loading conditions. Further research and field monitoring would support refinement and potential adoption into DOT practice.

CONTENTS

LIST OF TABLES

LIST OF FIGURES

1. INTRODUCTION

Buried three-sided structures must sometimes be supported on deep foundations. These are typically driven piles with a pile cap at the top. Currently, there is no method for distributing live load forces along the length of the foundation and down to the piles. Distribution of dead loads is also subject to some complexity, because of the effect of the interaction between group piles and the resulting different pile head stiffnesses on load transfer to the piles. Engineers then typically resort to judgment. As an example of how this might work, it would be overly conservative to assume that a live load would be entirely resisted by a single pile, but it would be unconservative to assume that all piles would resist the live load equally. This uncertainty can be more problematic for transportation infrastructure contracts in which the pile foundation configuration is estimated by the engineer of record (EOR), but the final design of the piling is the responsibility of the contractor. The EOR and contractor can make different assumptions as to the load distribution between piles.

This establishes the need to have a better understanding of live load distribution on deep foundations under buried three-sided structures. The main goal of the proposed research is to evaluate the live load distributions on deep foundations under buried three-sided structures and develop guidelines for the design of deep foundations for three-sided structures that the Indiana Department of Transportation (INDOT) and other transportation agencies may adopt. The goal will be achieved through realistic simulations of design conditions using finite element analysis (FEA) and realistic constitutive models. This research will summarize what the current practice is and the configurations and methods of construction of the various types of structures, present the analysis of a series of realistic simulation results, and further develop design guidance for the piles supporting three-sided structures.

1.1 Typical Configurations, Size and Foundation Design for Buried Three-Sided Structures

Buried three-sided structures are usually used as culverts or underpasses for pedestrians. They appear when either a stream or ditch flows across a road or when a safe crossway is needed for crossing traffic. They usually have wingwalls made of either precast or cast-in-place concrete.

There are two types of three-sided structures: flat top and arch top. A typical three-sided structure with a flat top is shown in Figure 1.1. Based on INDOT's previous experience with these structures, the span of the culverts—the perpendicular distance between two side walls—ranges from 18 ft to 60 ft; the longer dimension of the structure—the dimension perpendicular to the road that the structure crosses—ranges from 38 ft to 172 ft. Examples secured from INDOT of the general design and configuration of these structures are shown in Table 1.1. Table headings are related to the terms defined in Figure 1.1.

Buried three-sided structures are usually built on footings instead of piles, as discussed by the American Association of State Highway and Transportation Officials (AASHTO, 2020). But deep foundations must be used when either greater capacity than the footings can provide or scour protection is required. Discussion of specific design guidelines for foundations of culverts is scant at best. However, the Wisconsin Department of Transportation (WisDOT, 2021) mentions in its bridge design manual that either spread footings or pile-supported footings may be used for pedestrian underways, but that piles should be used for waterways for scour protection. Weak soil conditions also require pile support for these structures. The Minnesota Department of Transportation (MNDOT, 2013) provides a very specific directive that piles must be used if the thickness of unstable material below a footing is greater than 2 ft.

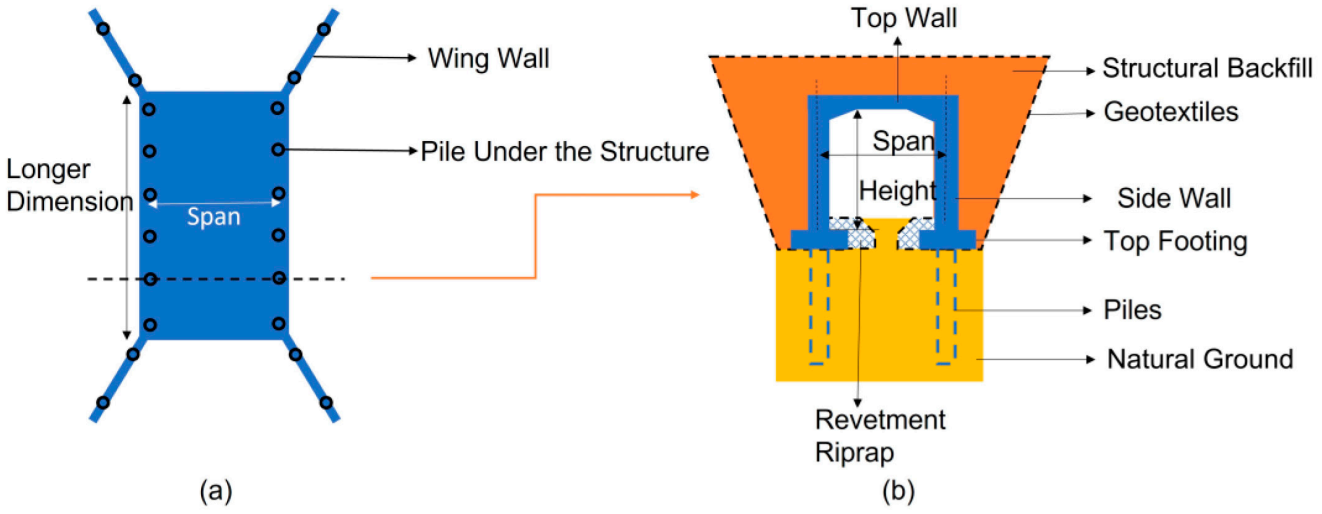

Figure 1.1 A Typical Configuration for a Buried Three-Sided Structure With Flat Top: (a) Top View of the Structure; (b) the Cross Section of the Structure.

TABLE 1.1
Information from Select INDOT Cases Involving Pile-Supported Three-Sided Structures.

No.	Span (ft)	Longer Dimension (ft)	Height (ft)	Pile Type; Pile Group Configuration; Spacing Between Piles (ft)	Design Capacity of Individual Piles (kips)	Comments
1	19	51	10	14-inch pipe pile; Single-row; 6.375	160	
2	18	64	8-12	HP 12 × 53 pile; Single-row; Not specified	234	
3	28	76	9	HP 12 × 53 pile; Single-row; 9.0	443	
4	24	58	11	HP 12 × 53 pile; Single-row; 5.0	200	Battered pile included. Arch top
5	52	172	14	HP 12 × 53 pile; three-rows; 4.0–6.0	449	
6	28	38	10	HP 12 × 53 pile; Single-row; Not specified	501	Skewed structure
7	40	55	9	HP 12 × 53 pile; Single-row; 10.0	434	Skewed structure
8	60	88	6	HP 12 × 53 pile; Single-row; 3.0–7.0	203	

Stem walls are also occasionally used to connect the footings or pile caps to the three-sided structure. This is usually the case when a taller structure is needed. The Washington State Department of Transportation (WSDOT, 2015), for example, provides in its guidance that a stem wall should be considered when the vertical culvert opening is beyond 10 ft in dimension. The difference between a structure bearing on a stem wall or directly on the footing is the position of the connection of the superstructure with the substructure, which is constructed in a way that would typically be modeled as a pin connection. In the case of footings without a stem wall, the structure is positioned inside a precast keyway on top of the footing and grouted there. These structures are later referred to as Type A structures. When a stem wall is used, the same type of connection is made at the top of the stem wall. These structures are referred to as Type B structures. The definitions of Type A and Type B structures are shown in Figure 1.2.

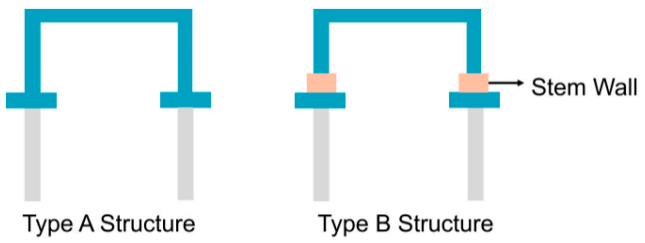

Figure 1.2 Type A and Type B Structures.

Despite the obvious need and the recurring use of pile-supported three-sided structures, the literature lacks reports of research on how to analyze or design piles supporting buried three-sided structures.

For this research, we performed a survey to investigate the most used configurations of the pile groups supporting the buried three-sided structures, and the most adopted state-of-practice design methods. Thirty-four geotechnical specialists from departments of transportation (DOTs) of different states participated in the survey. From this survey, we established the typical dimension of the buried three-sided structures and the pile groups supporting them, analyzed the current main concerns when designing the pile-supported-three-sided structures, and the current design methods for the foundations of the buried three-sided structures.

1.2 Sources of Loads

Many types of loads should be considered when designing a buried three-sided structure and its foundations. Dead loads on the foundations will obviously result from the weight of the structure and of the soil covering the structure, although the loads actually transferred to the piles will depend on the individual pile head stiffnesses, which will, in turn, depend on the foundation soil. Live loads are not as clearly obtained.

According to AASHTO (2020), a wheel load is modeled either as a concentrated point load or a uniformly distributed

pressure within the tire contact area. AASHTO (2020) also recommends that designers should follow the HL-93 model to decide the amplitude and the position of wheel loads. In the HL-93 model, the load distribution—that is, the arrangement of wheels and load per wheel—of a design truck is specified. The area of contact between the truck tires and the pavement is also specified. Knowing the distribution of the weight of the vehicles, the wheel load may be modeled as either a limited number of concentrated point loads, or an average distributed force acting on the area of contact between the tire and the road. However, in the design of buried culverts, complexities exist regarding the distribution of live loads. One such complexity is the transfer of live loads to the structure through soil. The distribution through soil of the wheel load applied at the top that reaches the structure is a question that needs to be addressed. Some studies have investigated the transmission of earth pressures to buried structures (Bennett et al., 2005; Dasgupta & Sengupta, 1991; Poulos & Davis, 1974), but these studies have either relied on simplification of material response, such as treating soil as an elastic material, or are based on limited test results.

1.3 Load Distribution in the Pile Group and Foundation Design

Research performed to study the load distribution between piles in pile groups—such as Han et al. (2020)—shows that the pile groups supporting bridge structures are subjected to uneven load distributions due to live loads and load eccentricities. Poulos & Mattes (1971) also suggested that the load distribution within a pile group with a rigid pile cap becomes less uniform when the stiffness of the piles increases.

As related to three-sided structures specifically, no literature was found regarding the transfer of loads—dead or live loads—to group piles. Guidance cannot be found in AASHTO (2020). This question of how to determine the loads to be carried by each pile in a group and how to design them is a major focus of this research. The research will also explore the difference in load transmission between Type A and Type B structures. This comparison may lead to a standardization of the use of Type B structures if advantages are revealed by the comparison.

Three-sided structures must be designed to prevent all identifiable limit states. A key limit state is differential settlement in the span direction of the three-sided structure, which may have reflection both on the roadway above and on the integrity of the three-sided structure itself. Relative movement of the culvert as a rigid body with respect to the roadway or surrounding media must also be contained. As always, bearing capacity failures must be prevented.

There are two main components of the load on the top of the pile head that we considered in this research. One is the vertical force; another one is the moment pointing inward to the center of the bridge, as shown in Figure 1.3. The total load carried by the buried three-sided structure will partly be absorbed by the soil and the backfill material, and the rest will be transferred to the piles. According to Y. Wang et al. (2022), the lateral moment added on a pile group will be mostly absorbed by the vertical displacement when there are multiple rows of piles in the pile group

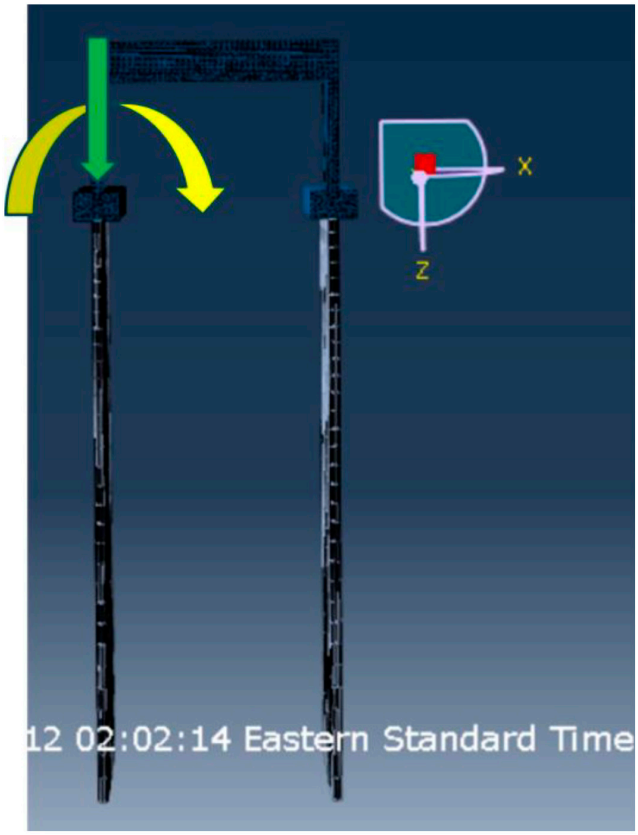

Figure 1.3 Two Components of Load Carried by the Piles Supporting the Three-Sided Structures.

along the direction of the moment but will all be transferred to the pile head when there is only one row of piles in the pile group. As we can see from Table 1.1, the pile groups supporting the culverts sometimes have multiple rows but often are single-row groups. Thus, moment distribution should also be considered.

1.4 Finite Element Analysis Used in Research of Buried Culverts

FEA has been used in recent years to investigate the mechanical behavior of buried culverts. Awwad et al. (2000) performed three-dimensional (3D) FEA for large-span concrete box culverts, projecting the wheel loads on the top of the culverts' slab using the ASTM C890 (ASTM, 1999) formula. In that research, the culverts are simulated using quadrilateral shell elements and the linear elastic constitutive model. The authors reached the conclusion that wheel loads will dominate the behavior of the box culverts when the earth cover depth is less than 3 ft, whereas the impact of the wheel loads is negligible when the earth cover depth exceeds 7 ft. Garg and Abolmaali (2009) and Pimentel et al. (2009) performed 3D FEAs of box culverts and compared the resulting load-deflection plot with that obtained from experiments. However, the soil on the top of the culvert was neglected. Wells (2016) performed two-dimensional (2D) FEA and studied how the soil elastic modulus, fill depth, span

length, culvert slab thickness, and asphalt pavement thickness affected the dynamic amplification of the live load above buried box culverts. Kadivar et al. (2018) performed 2D and 3D FEA of three-sided structures to study the impact of the mechanical behavior of the three-sided structures under dynamic live loads. Both studies assumed the load as a triangular pulse with a pulse duration equal to the time needed for a truck to pass the culvert. These studies assumed the soil to be an elastic material. Ramadan and El Naggar (2022) performed 2D FEAs of a three-sided structure supported by footings to investigate the current code and equation provided by AASHTO (2020). The soil was simulated using a Mohr-Coulomb model. Ozturk (2024) studied the dynamic behavior of three-sided underpass culverts under near-fault and far-fault ground motions using 2D FEA. The study analyzed how soil stiffness and seismic characteristics influence the structural response of these structures. Linear elasticity was assumed in the research. S. Wang et al. (2024) analyzed vertical earth pressure on hinged prefabricated box culverts using 3D FEA, employing an elastic model for culverts and a Mohr-Coulomb model for soil.

These publications relied on simple soil models that may not be sufficiently realistic and did not consider deep foundations as the foundations for the three-sided structures. In this research, we will use realistic constitutive models for soil and perform 3D simulations for three-sided structures bearing on deep foundations to bridge this knowledge gap.

1.5 Structure of this Report

This report will follow the following structure. In Chapter 2, we will summarize the survey results, in which 34 engineers from DOTs from all over the United States participated. We will establish the dimensions and the most popular configurations of the buried, pile-supported three-sided structure based on the survey results, and summarize the main concerns expressed by engineers involved in the design of the buried three-sided structures. We will also discuss details of the design methods used for the foundations of the three-sided structures. In Chapter 3, we will introduce the finite element configurations used to analyze the buried, pile-supported three-sided structures, which include the details of the dimensions of the model, boundary conditions of the model, constitutive model used to model the soil mechanical response, and the computation step set up in the simulation. In Chapter 4, we will perform parametric studies based on the simulation results. The chapter is organized by discussion of factors influencing the response of the structures, including the existence of a stem wall, the stem wall height, the earth cover depth, the shear key depth, the width of the segments of the three-sided structures, the location of the truck, and the soil profile. In Chapter 5, we will summarize the lessons learned from the simulation results, compare them with the traditional moment-of-inertia method calculations, and eventually propose design guidelines for deep foundations supporting buried three-sided structures. Finally, in Chapter 6, we will summarize the main conclusions of this report.

2. SURVEY RESULTS

A survey was conducted to document the current design practices for pile-supported buried three-sided structures. Thirty-four geotechnical engineers from various state departments of transportation across the United States participated in the survey. The survey identified key geometric parameters (dimensions) for typical three-sided structures, common connection methods between different components, primary design considerations among engineers, and frequently used design methods.

2.1 General Description

A total of 74% of the participants reported that pile-supported three-sided structures had been constructed in their respective states, while 26% indicated otherwise. According to the survey, these structures are chosen primarily due to concerns about scour and soil bearing capacity, economic reasons, and cases where an inverted slab or full slab is not feasible. However, in many situations, scour necessitates a full bottom slab, often the preferred solution when conditions are not ideal.

2.2 Design of Three-Sided Structures

Participants were asked to report the most commonly observed dimension ranges of pile-supported three-sided structures. The dimensions considered in this section include rise (height), span, length, and wall thickness, as shown in Figure 2.1.

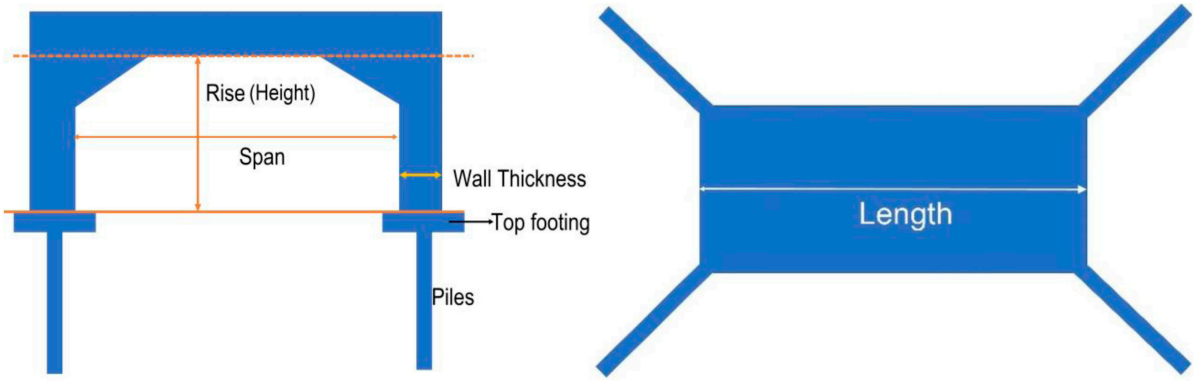

Figure 2.1 The Dimensions Considered in the Survey.

TABLE 2.1
The Dimensions Established From the Survey.

Dimensions	Minimum According to the Survey	Maximum According to the Survey
Rise	6 ft	12 ft
Span	10 ft	30 ft
Length	20 ft	80 ft
Wall thickness	8 in.	12 in.
Footing thickness	2.5 ft	3.5 ft
Pile diameter	12 in.	16 in.
Stem wall height	2 ft	6 ft

Responses varied across all provided options, indicating no strict size constraints for this type of structure. However, certain dimension ranges were more frequently selected. Table 2.1 summarizes the most common dimension ranges based on survey results.

According to the literature, buried three-sided structures are typically categorized into true-arch, arch-topped, and flat-topped. Participants were asked to estimate the relative prevalence of each type, and the results indicated that flat-topped and arch-topped structures are the most commonly observed, in that order. Additionally, some three-sided structures are skewed, meaning their length is not perpendicular to traffic direction. The survey revealed that most participants believe such structures appear in less than 50% of cases.

When asked about the primary loads considered in designing three-sided structures, participants most frequently reported earth pressure, live loading, and vehicular loading. Other loads, such as water buoyancy, hydrostatic pressure, and downdrag loading, were considered only when necessary.

Only 33% of the participants reported using FEA techniques in their design process. Among those who do, the most commonly used methods for simulating wheel loading include uniformly distributed pressure, concentrated static loads, and time-dependent moving loads.

The primary risks considered in designing three-sided structures include uplift, unbalanced loading in skewed structures extending through embankment slopes, foundation settlement, differential settlement between the structure and backfill, longitudinal differential settlement, top slab deflection due to live loads, and horizontal movement. The most frequently cited concerns were foundation settlement, longitudinal differential settlement, and top slab deflection due to live loads and horizontal movement. Additionally, only 23% of the participants reported considering dynamic allowances in their design process.

The depth of earth cover above buried three-sided structures significantly impacts their mechanical behavior. According to the survey, the most typical three-sided structures are buried under 4–8 feet of soil with a friction angle of 30–35 degrees. Based on AASHTO standards, live load distribution should generally be considered.

2.3 Design of Foundations

The first step in designing a foundation for a retaining structure is selecting the appropriate foundation type. Survey participants reported that pile-supported foundations are chosen when poor soil conditions, bearing capacity concerns, potential scour, environmental factors, or prohibitive depth to bedrock make shallow foundations impractical. Conversely, when adequate bearing capacity exists, competent soil is present, settlement is within allowable limits, the depth to bedrock is small, the structure size is moderate, or minimal scour is expected, shallow footings are generally preferred.

Economic factors also play a significant role in decision making. One participant noted that spread footings are typically used for nonwater crossings, while piled footings are preferred for water crossings. While shallow footings are the default choice, piled footings may be required when additional foundation capacity is needed.

H-piles and closed-ended steel pipe piles are the most commonly selected options when piled footings are used. Other foundation types, such as drilled shafts, concrete-filled closed-ended pipe piles, and micropiles, are occasionally used. The typical pile diameters range from 12–16 in., footing widths from 4–6 ft, and footing thicknesses from 2.5–3.5 ft.

The primary factors governing the design of footings for three-sided structures include the soil bearing resistance, total settlement, and differential settlement. Horizontal movement and sliding failure are also considered in some cases. The primary factors influencing pile design include nominal bearing resistance, horizontal movement, and total settlement. Participants reported that downdrag loads are typically considered in pile design, but not when defining loads acting on the buried three-sided structures themselves.

Single-row pile groups with a spacing of 2 to 5 times the pile diameter or the cross-section width of H-piles are the most commonly used for pile group configurations. Two-row pile groups are occasionally used, while multirow configurations with more than three rows are uncommon.

The connection between the footings and the three-sided structure often involves a stem wall. According to survey responses, the stem wall is typically connected to the footings using reinforcing bars, which suggests that the stem wall and footings can be treated as a single unit in numerical simulations. However, the connection between the stem wall and the three-sided structure often includes a shear key, which may introduce moment transfer discontinuities.

2.4 Wingwall Design

Buried three-sided structures are often constructed with wingwalls. The survey included questions to capture the current design practices for wingwalls.

The selection of wingwall foundation types follows similar considerations to those for the three-sided structures. However, participants also preferred maintaining consistency between the foundation types of the buried structure and the wingwall.

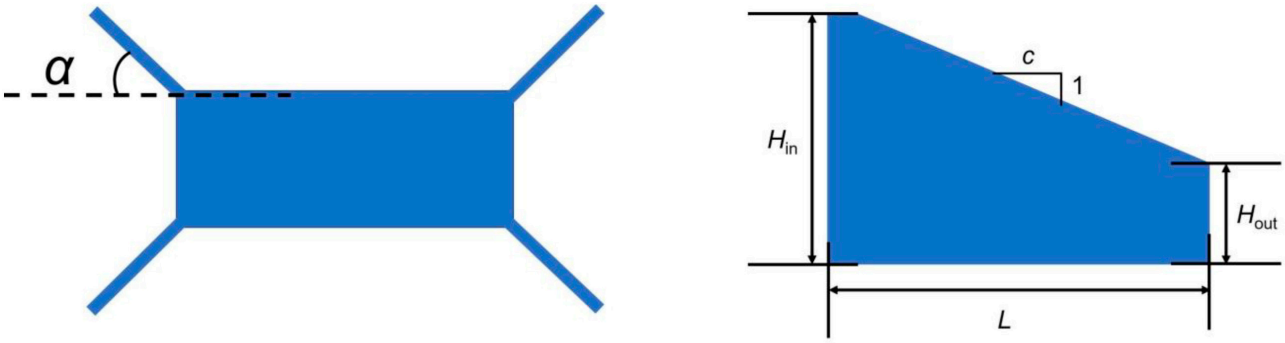

Figure 2.2 The Wingwall Dimensions Considered in the Survey.

TABLE 2.2
Dimensions of the Wingwalls Established From the Survey.

Dimensions	Minimum According to the Survey	Maximum According to the Survey
H_{in}	9 ft	11 ft
H_{out}	3 ft	5 ft
c	2	3
L	10 ft	15 ft
α	30°	45°

Figure 2.2 shows the typical dimensions of wingwalls, while Table 2.2 summarizes the most commonly observed size ranges.

2.5 Key Findings from the Survey

The survey results established the key geometric parameters of buried three-sided structures, their foundations, and their wingwalls. The findings indicate that flat-topped and arch-topped structures are the most commonly used. H-piles and closed-ended pipe piles are frequently chosen when piled footings are required. Piles are selected due to poor soil conditions, environmental considerations, economic factors, differential settlement concerns, and the potential for scour. Additionally, the survey revealed that, while the connection between the stem wall and footings is typically reinforced with bars (allowing them to be treated as a single unit in numerical models), the connection between the stem wall and the three-sided structure itself is often achieved through a shear key, which may introduce moment transfer discontinuities. Finally, the foundation selection process for wingwalls follows similar principles to that of the three-sided structure itself, with additional consideration given to consistency between the two.

3. SIMULATION SETUP

We performed 12 3D FEAs of pile-supported, buried three-sided structures to investigate the potential factors that have an impact on the live load distribution among the piles in the pile group supporting the whole system. The model includes the structure itself, the foundation system (including the top footings and the piles), the low-strength flowable backfill surrounding the structure, the soil surrounding the piles, the earth cover above the structure, and the asphalt pavement on top of the whole system. Wingwalls are not considered due to geometric complexity. The scenarios considered in this study cover a variety of soil profiles, earth cover depths, shear key depths, stem wall heights, truck positions, pile tip conditions, and segment widths. The simulations were performed using Abaqus/Explicit 2024 (Dassault Systèmes, 2024). Detailed information on the simulations included in this study is summarized in Table 3.1.

3.1 Geometry

Figure 3.1 shows an example of the simulation. In Figure 3.1, the piles are entirely buried in a uniform normally consolidated (NC) clay layer, so they are not visible externally. The three-sided structure is wrapped in low-strength flowable backfill material. A loose Ottawa sand layer with a relative density of 40% surrounds the structure wrapped by the backfill material. Below the sand layer, the piles and the footings can be embedded in different soil profiles. The considered soil profile consists of uniform NC clay, over-consolidated (OC) clay over NC clay, and NC clay over sand. Specifically, the soil immediately below the pile tip is replaced by a competent dense sand layer with a relative density of 80% for the end-bearing pile scenario. The term "earth cover" refers to the layer of dense sand (modeled using the properties of the well characterized Toyoura sand) that directly covers the structure. In some cases, there may be a sand layer cover on top of the three-sided structure before the pavement material is placed on it. This layer is typically less than 4 ft thick. In our research, we considered 0.31 m, 0.61 m, and 1.22 m (1 ft, 2 ft, and 4 ft) of earth cover depth. Above the earth cover, an asphalt layer lies on top of the whole system to simulate the road surface. The depth of the asphalt layer is always 0.17 m (6.5 in.).

The piles are closed-ended pipe piles, which is one of the most popular options selected by engineers across the country. The pile diameter is 0.305 m (12 in.), the wall thickness is 0.009 m (0.35 in.), and the pile length is 20 m (66 ft). The footings are 1.5 m (5 ft) in width and 0.9 m (3 ft) in depth and are considered entirely embedded by the soil. There are ten piles under each footing, and the pile spacing is four times

TABLE 3.1
Simulations Involved in this Research.

No.	Soil profile[1]	End-Bearing?[2]	Shear Key Type[3]	Stem Wall Height	Segment Width[4]	Pile Length	No. of Trucks and Position[5]	Earth Cover Depth[6]
1	NC Clay	Yes	Deep	0	10 ft	66 ft	Close to one side of the road/1	1 ft
2	NC Clay	No	Deep	0	10 ft	66 ft	Close to one side of the road/1	1 ft
3	NC Clay	No	Deep	6 ft	10 ft	66 ft	Close to one side of the road/1	1 ft
4	NC Clay	No	Deep	3 ft	10 ft	66 ft	Close to one side of the road/1	1 ft
5	NC Clay	No	Shallow	6 ft	10 ft	66 ft	Close to one side of the road/1	1 ft
6	NC Clay	No	Shallow	0	10 ft	66 ft	Close to one side of the road/1	1 ft
7	NC Clay	No	Deep	0	5 ft	66 ft	Close to one side of the road/1	1 ft
8	NC Clay	No	Deep	0	10 ft	66 ft	Close to one side of the road/1	2 ft
9	NC Clay	No	Deep	0	10 ft	66 ft	Close to one side of the road/1	4 ft
10	NC Clay	No	Shallow	0	10 ft	66 ft	At the center of the road/1	1 ft
11	NC Clay	No	Shallow	0	10 ft	66 ft	Close to both sides of the road/2	1 ft
12	OC[7] over NC Clay	No	Shallow	0	10 ft	66 ft	Close to one side of the road/1	1 ft

[1] "Soil profile" refers to the soil surrounding the piles and the footings, extending from the structure down to below the pile tip.
[2] For the end-bearing scenario, the soil immediately below the pile is replaced by a layer of dense sand with a relative density of 80%.
[3] The details of the shear key can be found in Chapter 3.1.
[4] "Segment width" refers to the dimension of the segment in the direction of the structure length. See Chapter 3.1 for details.
[5] The road is designed to have two lanes, one for each direction. Trucks are always parallel to the span of the three-sided structure.
[6] The details for earth cover depth can be found in Chapter 3.1.
[7] OC: over-consolidated.

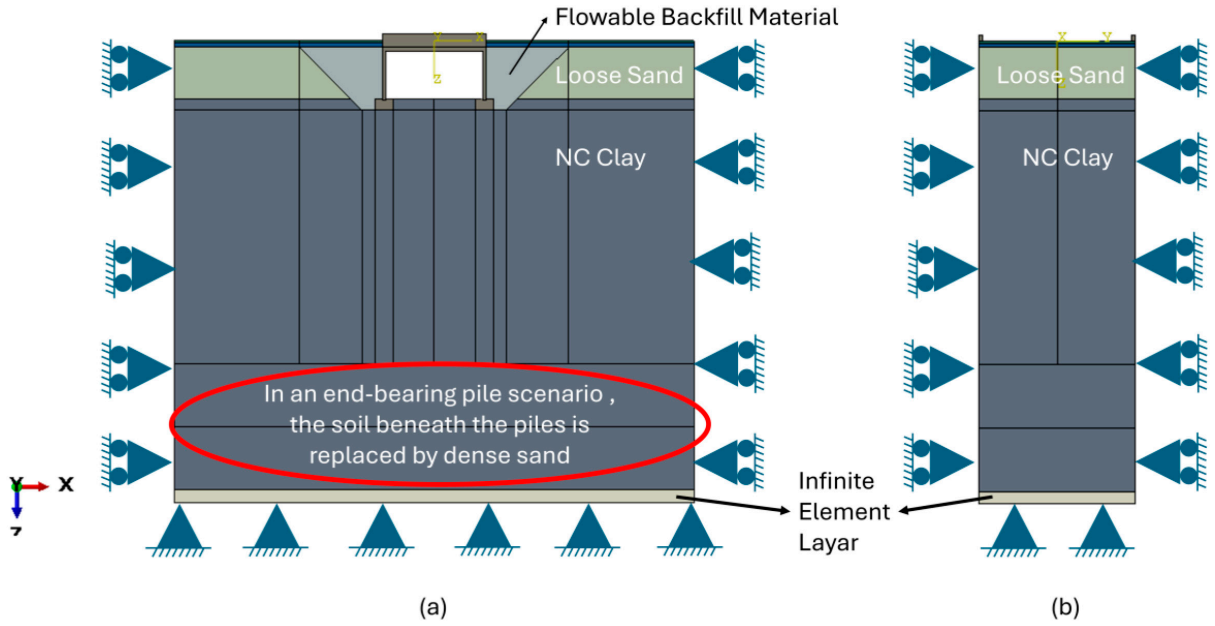

Figure 3.1 Example of the Simulation With Piles Embedded in NC Clay With (a) Front View and (b) Side View.

the pile diameter. Typically, riprap is placed on the corner of the structure to stabilize the whole system. We replaced this component with a uniformly distributed pressure added on the exposed top of the footing. This footing size lies in the typical range used for footings to support buried three-sided structures. Figure 3.2 presents two views of the foundation system. In Figure 3.2a, the piles, footings, and the structure supported by the footings are clearly visible because the surrounding soil and extraneous materials have been removed. In Figure 3.2b, the complete model is shown from the front, with the piles entirely buried in the soil. This side-by-side display helps to illustrate the size of the piles and their position within the soil.

The structure selected for the analyses is medium-sized according to the survey results. The height of the structure, measured from the inner upper bound of the structure to the top of the soil layers inside the structure, is 3.8 m (12.5 ft). The span of the structure is 7.8 m (25.6 ft), and the length of the structure is 12.1 m (39.7 ft). The thickness of the wall is 0.3 m (1 ft). A structure with these dimensions can have two lanes of traffic on top of it, with one lane for each direction. The three-sided structure is divided into several segments

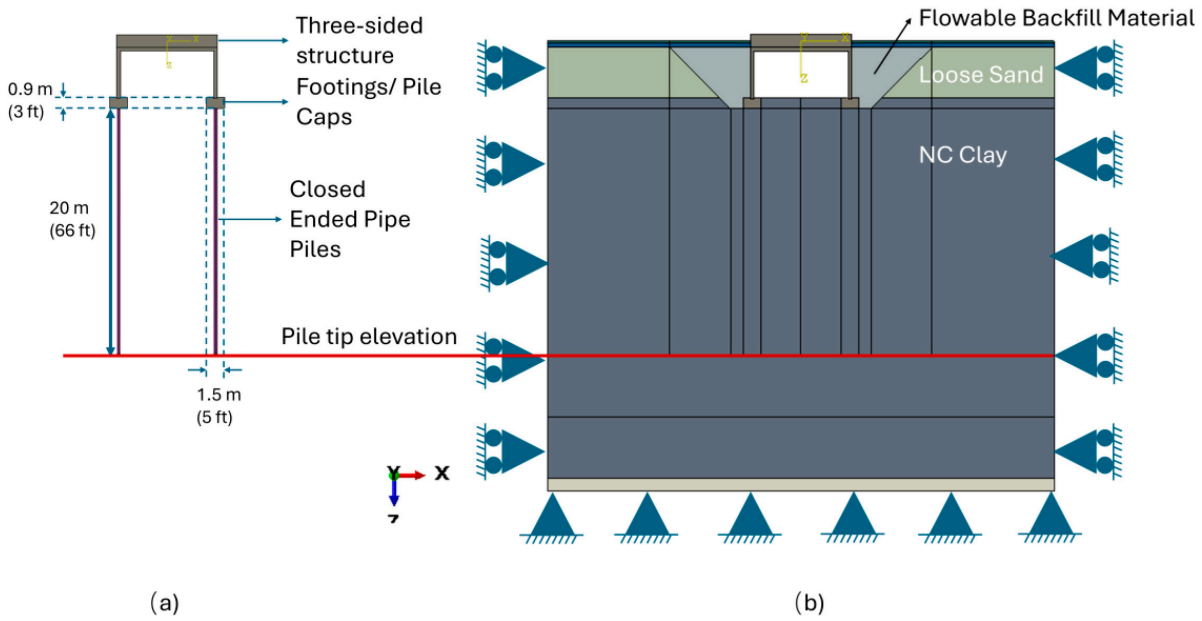

Figure 3.2 Exposed and Embedded View of the Foundation System: (a) Exposed View of the Piles, Footings and the Supported Structure With the Surrounding Soil and Extraneous Materials Removed; (b) Front View of the Complete Model, Where the Piles are Fully Embedded in the Soil.

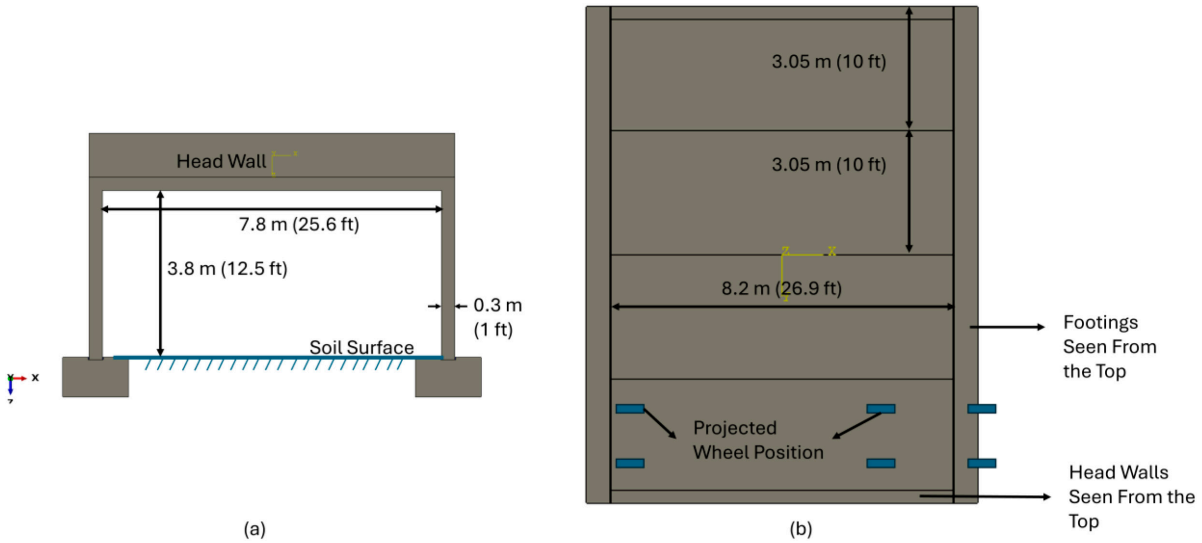

Figure 3.3 A Simulated Three-Sided Structure: (a) Front View With All Dimensions Labeled; (b) Plan View With the Projected Positions of the Truck Wheels.

along its length. The width of these segments, measured along the structure's length, is typically between 5 ft and 10 ft. This study simulates both 10-ft segment scenarios and a 5-ft segment scenario. When segments are 10 ft wide, a standard HL-93 truck can be placed entirely on one segment. However, if the segments are only 5 ft wide, the truck's two rows of wheels will be placed on two adjacent segments. Figure 3.3 shows a simulated three-sided structure divided into four 10-ft wide segments. Figure 3.3a displays the front view of the structure, with all the dimensions labeled. Figure 3.3b presents the plan view of the structure, with the projected positions of the truck wheels marked on it, indicating where the truck will be placed on the roadway.

For a Type B structure specifically, the stem wall height is either 3 ft or 6 ft. These two different heights are considered for investigating the impact of the stem wall height.

The shear key connecting the structure with either the footing or the stem wall is modeled in two ways, shown in Figure 3.4 as a shallow or deep shear key. A deep shear key is 0.2 m (7.8 in.) in depth and 0.3 m (11.8 in.) in width. There is no friction between

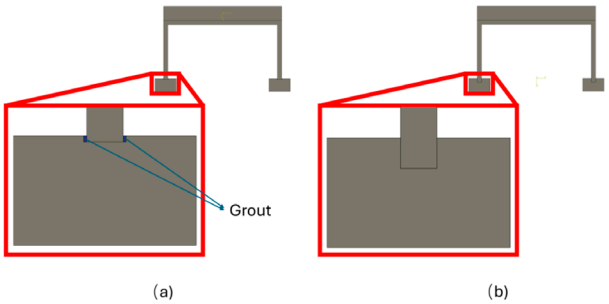

Figure 3.4 Deep Shear Key and the Shallow Shear Key Simulated in This Research: (a) Shallow Shear Key; (b) Deep Shear Key.

the footing and the structure. A shallow shear key is 0.05 m (2.0 in.) in depth and 0.35 m (13.8 in.) in width. For the shallow shear key, there is a 0.025 m (1.0 in.) wide grout strip between the structure and the footing. The grout strip is modeled as a low-stiffness elastic strip directly attached to the footings. The contact surface between the grout and the structure is modeled using tied nodes, whereas the bottom of the structure and the inner boundary of the shear key is frictionless.

Most of the dimensions mentioned above initially came from a real case design sheet and were later adjusted slightly to align with the survey results.

3.2 Material

The piles are made of steel with a Young's modulus of 200 GPa (29007.5 ksi). However, in our model, the piles are simulated as solid cylinders instead of pipes. To do that, the Young's modulus of the piles is adjusted so that their bending stiffness matches that of a pipe pile with a wall thickness of 0.009 m. The converted Young's modulus is 29.2 GPa (4235.1 ksi). The void ratio is considered as 0.2. The unit weight of the pile is set to be the same as the unit weight of the soil surrounding it. We assume that the self-weight of the pile is already balanced by the earth stress generated during the installation process.

The structures are usually made of concrete, which has a unit weight of 22.6 kN/m3 (143.8 pcf). This material is modeled as elastic, with a Young's modulus of 25.1 GPa (3640 ksi). The void ratio is considered 0.3.

The low-strength flowable backfill and grout are also modeled as elastic materials, with Young's modulus of 22.1 MPa (3.2 ksi) and 300 MPa (43.5 ksi) and void ratios of 0.2 and 0.3, respectively.

The advanced two-surface constitutive models for both sand and clay are used to model the soil mechanical behavior. The parameters can be found in Chakraborty et al. (2013) and Loukidis and Salgado (2009). Boston Blue clay (BBC) is used in simulations. The loose sand layer surrounding the structure and the other sand layers surrounding the footings and the piles, or beneath the piles, are modeled as Ottawa sand. However, the earth cover is usually very dense sand with angular particles, so it is modeled as Toyoura sand with a relative density of 90%, because the properties of Toyoura sand best match it.

3.3 Boundary Conditions

The boundary conditions were shown previously in Figure 3.1. The four sides of the model are considered fixed in the direction perpendicular to the boundary surface. This assumption is reasonable because, in practice, the soil domain is unbounded, and this is reasonably modeled by a boundary that is sufficiently removed from the structure but provides sufficient horizontal support. The wingwalls also provide sufficient support to prevent the structure from vibrating horizontally.

The whole model sits on a thin layer of infinite elements. The infinite element in Abaqus/Explicit is used to simulate the boundary that should be positioned infinitely far away for an unbounded domain. This type of element is naturally equipped with a fixed boundary condition on the open side (the side that is not directly attached to the model). The stress inside the infinite element consists of two components. The first component is a static stress component. The magnitude of this static stress component is calculated in the initial step of the simulation, to balance the predefined stress field inside the model. The second component is a damping term proportional to the velocity of the nodes on the closed side (the side where the infinite elements share the nodes with the rest of the model). The coefficients of the damping terms are calculated from soil Young's modulus and void ratio values input by the user. Here, we use Young's modulus of 18.5 MPa and void ratio of 0.2. These values are approximately equal to the average small-strain modulus of the loose Ottawa sand layer surrounding the three-sided structure, which is good enough to absorb the excessive wave generated in the live loading step.

3.4 Contact Involved in the Simulation

The finite element model was divided into several "parts." A "part" in Abaqus is simply a region in space that is occupied by a body or bodies that are subdivided into finite elements; if there is more than one body (a "component" of the part), the common boundaries of these bodies share nodes. The components integrated in the same part are connected, sharing nodes, which means that there will be no slip between the two components that are connected this way. For example, in our model, the piles are buried in the clay layer, so the clay and the piles can be represented in the same part, in which case the elements at the boundary of the piles share nodes with surrounding clay layer elements. The stress field is also considered continuous within the same part.

The asphalt layer on the top, the earth cover, all the soil layers beneath the road, the piles buried in the soil, and the flowable backfill material are all included in one part, namely part 1. Each footing is individually an independent part and is placed right on the piles. Although modeled as separate parts, the displacement degrees of freedom of the nodes on the footing surface are strictly tied to the degrees of freedom of nodes on the surface of part 1 that is in contact with the footings, following the assumption that the friction between the footings and the adjacent soil, piles or backfill material is infinitely

large. For the Type B structures, the stem wall and the footing are integrated into one part, following the survey results. The three-sided structure itself is built in several segments aligned along the length of the structure, as shown in Figure 3.3. Each segment is considered an independent part. The contact between the segments is considered frictionless. For the deep shear key scenario, the contact between the segment and the footing within the keyway is also considered frictionless. However, for the shallow shear key scenario, we model two grout strips in it that stitch the structure and the footing together, leaving only the bottom surface of the segment in frictionless contact with the footing surface. Considering that the flowable backfill is usually poured in place after the excavation and the placement of the structure is done, it is reasonable to consider the outer surface of the segments tied to the flowable backfill material with infinitely large friction. The top surface of the segments is also considered strictly stuck to the earth cover to avoid separation and stress discontinuity.

3.5 Meshing

The types of elements used in the simulation include the C3D8R element and the CIN3D8 element. The C3D8R element is the regular 8-node linear stress element equipped with reduced integration and an hourglass control technique. The CIN3D8 element is the infinite element used as the bottom boundary of the model. The minimum dimension of the element is 0.15 m. The finest elements are located in the zone of the asphalt layer where the wheel load is applied, the earth cover (which is directly above the structure), and the soil that is very close to the pile. Figure 3.5 displays an example of a typical mesh configuration for the simulations in this research.

3.6 Steps and Loads

The simulation has three steps: (1) the geostatic step, (2) changes in constraints and loading to reproduce the configuration of the structure before traffic loading, and (3) loading.

Before the simulation starts, we need to input an initial stress field to avoid a zero-stress state for the soil elements. The magnitude of the initial stress at a certain depth is estimated as the total stress in the soil at that elevation in an area far from the three-sided structure, that is, free-field stresses. We always assume the water table to be at the same level as the top of the footing so that the entire foundation system of the structure is submerged in water to simulate a river-crossing scenario. This scenario is more vulnerable compared to the scenario in which the buried three-sided structure is built across a pedestrian pathway.

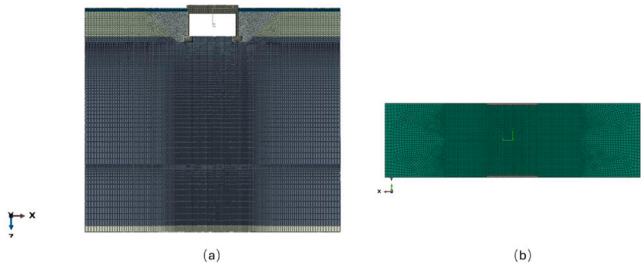

Figure 3.5 An Example of Mesh Configuration for the Simulations Involved in this Study: (a) Front View; (b) Plan View.

The first step is the geostatic step, which lasts for a computation time of 0.5 s, in which gravity is applied to the whole system. The clay layers are simulated under fully drained conditions. Consolidation is allowed to develop very fast but still reflects the long-term soil mechanical behavior. We intentionally do not consider intermediate consolidation states—that is, the transient phase of excess pore water pressure dissipation—because our objective is to quickly achieve a geostatic state rather than model the lengthy process of water dissipation, which is not critical for our analysis. To ensure that the gravity-induced stress field matches our initial conditions, we simultaneously apply two measures. First, we impose a uniform pressure on the top surface of the soil within the structure. This pressure is set equal to the total vertical stress in the soil outside the structure at the same elevation, which replicates the natural vertical stress distribution under free field conditions. Secondly, we enforce lateral displacement constraints along the inner sides of the three-sided structure to prevent horizontal movement and avoid any stress relaxation around the center space. Together, these actions maintain a consistent geostatic state across the model.

In the second step, we gradually release the uniform stress applied to the soil within the structure while simultaneously applying a uniform pressure on the exposed top of the footings. This additional stress, with a magnitude of 17.8 kPa (0.37 ksf), is equivalent to the pressure generated by the weight of the riprap. The lateral constraint is also removed during this step. All these changes occur gradually over a computation time of 1 s, followed by an additional 2 s for the system to adjust itself.

The third step is the loading step. The live loading usually occurs very fast, so the clay layers are loaded under an undrained condition in the loading step. We first switch the drainage condition of the clay layers from drained to undrained, and then 1 s of computation time is allowed for the system to adjust itself. After that, one or two trucks are gradually placed on the road. The truck load simulation follows the HL-93 model, where the load of the truck is modeled as uniformly distributed pressure across the tire contact area. The HL-93 model also specifies the magnitude of the pressure and the size of the tire area. The details of the HL-93 model are shown in Figure 3.6. When applying pressure to the top surface of the model, Abaqus distributes the pressure as nodal forces, which means that the live load could vary according to mesh configuration. To address this, we scale the live load pressure in each simulation so that the total applied load matches the load of either one or two HL-93 trucks.

4. PARAMETRIC STUDY

From each simulation, we extract three key load-related variables for the foundations of the structure: (1) the live load—defined as the difference in the load on each pile before and after the truck was placed on the road; (2) the live load moment—defined as the difference in the total moment on each pile before and after the truck was placed on the road; and (3) the cap

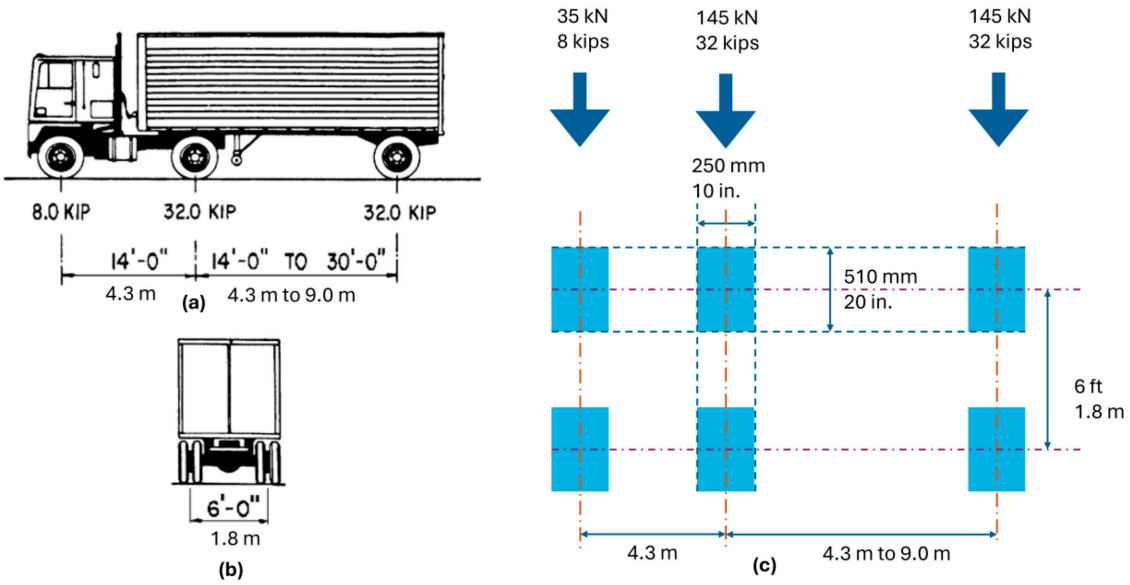

Figure 3.6 The Details of the HL-93 Model: (a) Side View of an HL-93 Truck; (b) Back View of an HL-93 Truck; (c) Details of the HL-93 Truck Tire Contact Area.

contributions—specifically, the cap base resistance, defined as the support provided by the soil directly beneath the pile cap. These results are presented systematically in this chapter.

4.1 Design Verification and General Overview

We first validated our simulation model against an actual design sheet. The design loads are specified as 1332 kips (5925 kN) on one of the pile groups and 1358 kips (6041 kN) on the other, which implies an average pile load of 133.2–135.8 kips (592.5–604.1 kN). Table 4.1 summarizes the dead load values extracted from the finite element analyses (FEAs) for scenarios in which piles are embedded in uniform NC clay, with variations that consider whether the pile tip bears on a competent sand layer and whether the highest stem wall is attached to the footings. The dead loads presented in Table 4.1, corresponding to the scenarios displayed in Table 3.1, range from 165–185 kN per pile.

In our design calculations, we employed both the Purdue Pile Design Method (PPDM; Salgado, 2022) and the AASHTO approach. Specifically, the AASHTO methodology incorporates the alpha, beta, and lambda methods to determine shaft resistance while providing a single method for calculating base resistance. Two options were considered for defining the soil profile:

1. The soil profile from the center of the bridge is used, with the top of the soil surface assumed to be at the same level as the top surface of the footings and the soil treated as normally consolidated.
2. The same soil profile is used, but the soil is assumed to be over-consolidated. This assumption is based on the consideration that the passageway below the bridge may have been created by excavation. In this case, the pre-consolidation stress is taken as equivalent to the vertical effective stress at the corresponding depth outside of the bridge.

TABLE 4.1
Dead Load Values Extracted From the Simulation Results.

No.	End-Bearing?	Structure Type (Type A/Type B)	Shear Key Depth (Shallow/Deep)	Dead Load Per Pile (kN)
1	Yes	Type A	Deep	164.9 (37.1 kips)
2	No	Type A	Deep	165.1 (37.1 kips)
3	No	Type B	Deep	177.8 (40.0 kips)
6	No	Type A	Shallow	185.5 (41.7 kips)
5	No	Type B	Shallow	182.9 (41.1 kips)

The calculated results are summarized in Table 4.2.

Comparison of the calculated design capacities, the values reported on the design sheet, and the FEA simulation results indicate that the piles are conservatively designed. It is important to note that the selected soil profile represents a worst-case scenario—piles embedded entirely in NC clay. In practice, piles are likely to be embedded in layered soils, with stronger layers yielding higher real capacities than those calculated here. Even when the piles are not end-bearing piles, the computed ultimate capacity typically exceeds the required design load and is at least 80% greater than the dead load determined from FEA. In end-bearing cases, the ultimate capacity increases dramatically, far surpassing the required design load. These findings suggest that the foundations of the three-sided structure may be over-designed in some instances.

Another load component of interest is the moment transferred to the piles. This moment arises from the presence of the central space within the bridge where no soil is present. The soil beside the structure pushes the side wall inward, while the weight of the road and its base forces the top slab downward, causing the side walls to move outward. According to our

TABLE 4.2
Design Check for the Simulated Scenarios.

Soil Profile Selection	Method	Shaft Resistance (kN)	Base Resistance (kN)	Ultimate Capacity (kN)
NC Clay (floating pile) Option 1	PPDM	462 (104 kips)	28 (6 kips)	490 (110 kips)
	α method	334 (75 kips)	22 (5 kips) [i]	354 (80 kips)
	β method	600 (135 kips)	22 (5 kips) [i]	622 (140 kips)
	λ method	546 (123 kips)	22 (5 kips) [i]	568 (128 kips)
OC Clay (floating pile) Option 2	PPDM	733 (165 kips)	39 (9 kips)	772 (174 kips)
	α method	542 (122 kips)	30 (7 kips) [i]	572 (129 kips)
	β method	750 (169 kips)	30 (7 kips) [i]	780 (176 kips)
	λ method	660 (148 kips)	30 (7 kips) [i]	690 (155 kips)
NC Clay (end-bearing piles) Option 1	PPDM	462 (104 kips)	679 (153 kips)	1142 (256 kips)
	α method	334 (75 kips)	1232 (277 kips) [ii]	1566 (356 kips)
	β method	600 (135 kips)	1232 (277 kips) [ii]	1832 (412 kips)
	λ method	546 (123 kips)	1232 (277 kips) [ii]	1778 (400 kips)
OC Clay over Dense sand (end-bearing piles) Option 2	PPDM	733 (165 kips)	679 (153 kips)	1413 (318 kips)
	α method	542 (122 kips)	1232 (277 kips) [ii]	1774 (399 kips)
	β method	750 (169 kips)	1232 (277 kips) [ii]	1982 (446 kips)
	λ method	660 (148 kips)	1232 (277 kips) [ii]	1892 (425 kips)

[i] Number calculated using method in AASHTO
[ii] Number calculated using Nordlund method

analysis, the dead load moment, generated by both soil pressure and the self-weight of the structure, acts toward the center of the bridge. Detailed values are provided in Table 4.3. As shown, the pile group supporting the Type A structure with a deeper shear key carries the highest moment, whereas a shallower shear key results in lower moments. Additionally, stem walls reduce the dead load moment transferred to the piles due to the irregular footing shape and the extra lateral resistance they provide. In this chapter, a moment bending the piles toward the center of the bridge is considered positive, and a moment bending them outward is considered negative.

4.2 The Effect of the Depth of the Shear Key

To study the effect of the depth of the shear key, we compared two pairs of simulations. The first pair—simulation No. 2 and No. 6—examines a floating-pile-supported Type A structure with a deep shear key versus a shallow shear key. The second pair—simulation No. 3 and simulation No. 5—examines a floating-pile-supported Type B structure with a 6-ft-high stem wall attached to the footings with deep or shallow shear key configurations. These simulations are labeled according to Table 3.1.

TABLE 4.3
Average Dead Load Moment Per Pile for Various Structural Configurations.

Type of Structure	Shear Key Depth (Deep or Shallow)	Average Dead Load Moment Carried by Each Pile Individually (kN·m)
Type A	Deep	51.02 (37.6 kips·ft)
Type A	Shallow	30.79 (22.7 kips·ft)
Type B (6-ft high stem wall)	Deep	39.43 (29.1 kips·ft)
Type B (6-ft high stem wall)	Shallow	32.75 (24.2 kips·ft)

All the simulations in this section are large-segment cases, which means the segment width selected in this section is 3.05 m (10 ft), which is sufficient for each segment to independently support a tri-axle truck. For all the simulations involved in this section, the truck is placed closer to one side of the road. Figure 4.1 shows the plan view of the segmented structure, and the piles beneath it. In this figure, the materials above and surrounding the structure have been removed to present the relative position of the truck and the structure. The projected positions of the two lines of truck wheels are shown in Figure 4.1.

The piles beneath each footing are numbered along the direction of the bridge's longer span to distinguish them. As illustrated, truck wheels will be solely supported by segment 4, and the piles numbered 8, 9, and 10 beneath each footing are expected to carry a greater fraction of the truck load. The pile numbering system is further detailed in Figure 4.2, in which the footings are also numbered based on their position. Figure 4.3 presents a front view of the entire model, with the position of the three axes of truck wheels marked using blue arrows. This figure shows that the truck is almost centered on the bridge, though its gravity center is slightly closer to Footing #1.

Figure 4.4 shows the live load distribution for the pile groups under Footings #1 and #2. Graphs in the same row correspond to the pile group supporting the footings on the same side. Graphs in the same column present results from the same simulation. As shown, piles 1, 2, and 3 make no contribution to carrying the live load, whereas piles 8, 9, and 10 carry most of the live load, as expected. This non-uniform distribution results from the

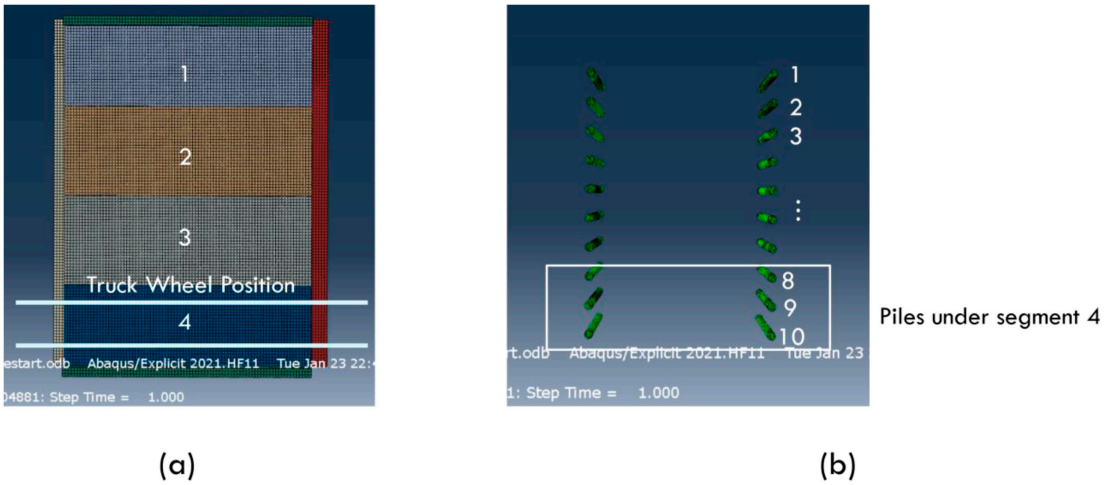

Figure 4.1 The Plan View of the Three-Sided Structure and the Piles Supporting the Structure: (a) the Three-Sided Structure With Projected Truck Wheel Position; (b) the Piles Supporting the Three-Sided Structure Labeled With Numbers.

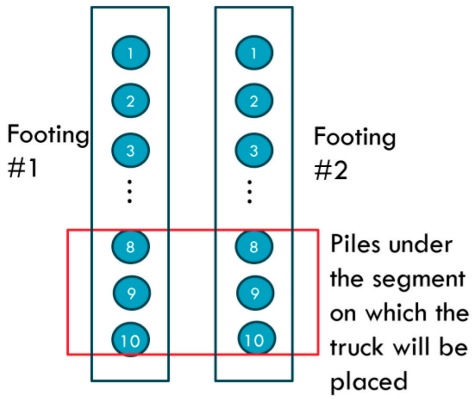

Figure 4.2 Schematic of the Pile and Footing Numbering System.

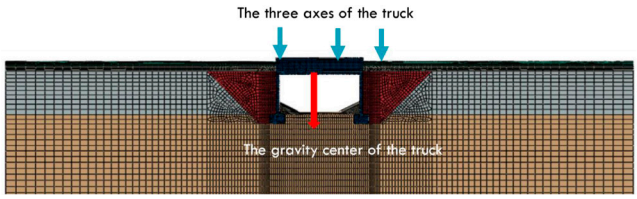

Figure 4.3 Frontal View of the Model With the Position of the Axes of the Truck and the Center of Gravity of the Truck Marked on the Graph.

assumption of no friction between segments. The maximum live load on a single pile reaches approximately 28 kN (6.3 kips). Overall, these results indicate that the shear key depth has little effect on the live load distribution.

For the Type B structure, the live load distributions for both deeper and shallower shear key configurations are shown in Figure 4.5. As before, the results confirm that shear key depth has only a slight effect on the live load distribution.

As for live load moment, the distribution among the piles supporting Type A structure is shown in Figure 4.6. The figures are arranged in the same way as Figure 4.4. By comparing figures in the same row, we observe that the magnitude of the moment increment is significantly smaller in the shallower shear key case than in the deeper shear key case. This indicates that the shallower key setup behaves more like an ideal pin connection, transferring force without moment.

Additionally, the direction of the moment increment differs between the two configurations. With a shallower shear key, the moment increment is negative, while with a deeper shear key it is positive. This indicates that, when a deeper shear key is used, the side walls are effectively locked to the footings or stem walls, and the moment increment caused by placing the truck bends the piles inward toward the center of the bridge as the footing and side walls rotate together. In contrast, with a shallower shear key, the moment increment is directed outward relative to what is observed when no truck is present, meaning that the side walls move outward, and the footing rotates accordingly. The higher stem wall case exhibits the same trend, as shown in Figure 4.7.

We also analyzed the cap contribution. Table 4.4 shows both the cap base resistance (i.e., the resistance provided solely by the soil beneath the cap) and the load transferred to the pile group, measured before and after the truck is placed on the road. The difference between the load values at these two time points represents the live load contribution.

Our analysis shows that the cap resistance accounts for approximately 10% of the total live load transferred to the base of the footing, regardless of the shear key type. This observation also holds true for high stem wall cases, but it is applicable only to the soil conditions around the cap that were studied here.

4.3 Multiple Truck Loading Analysis

We further compared simulation results for a Type A structure (with a shallow shear key) under single- and two-truck loading conditions—simulation No. 6 and simulation No. 11 in Table 3.1.

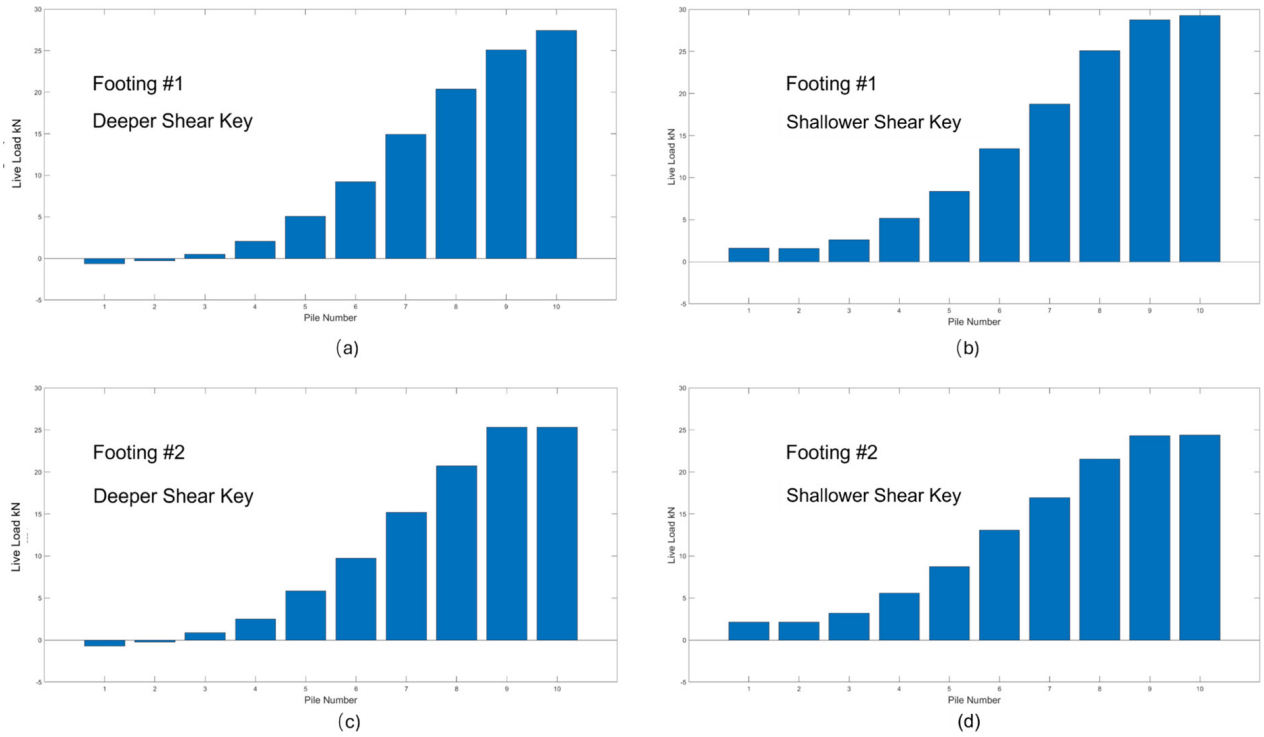

Figure 4.4 Live Load Distributions for Type A Structure With Floating Piles Embedded in NC Clay: (a) Pile Group Under Footing #1 With Deeper Shear Key; (b) Pile Group Under Footing #1 With Shallower Shear Key; (c) Pile Group Under Footing #2 With Deeper Shear Key; (d) Pile Group Under Footing #2 With Shallower Shear Key.

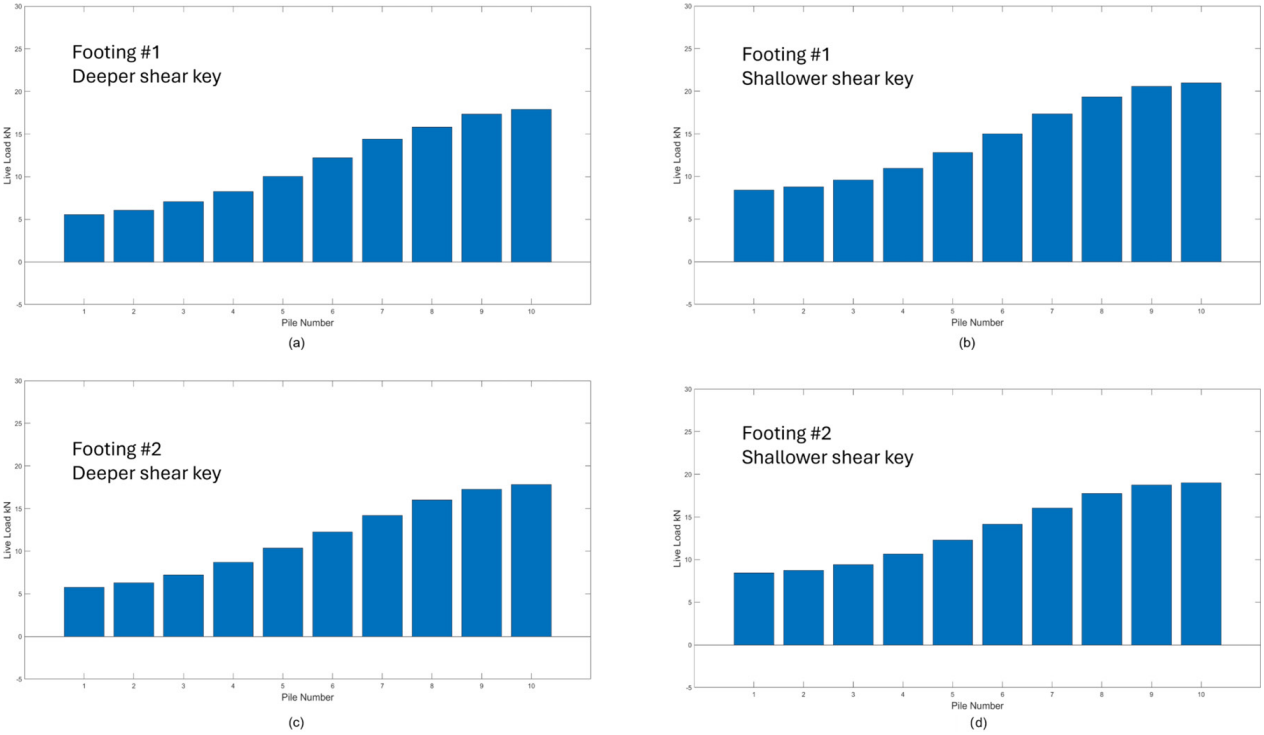

Figure 4.5 Live Load Distributions for Type B Structure With Floating Piles Embedded in NC Clay: (a) Pile Group Under Footing #1 With Deeper Shear Key; (b) Pile Group Under Footing #1 With Shallower Shear Key; (c) Pile Group Under Footing #2 With Deeper Shear Key; (d) Pile Group Under Footing #2 With Shallower Shear Key.

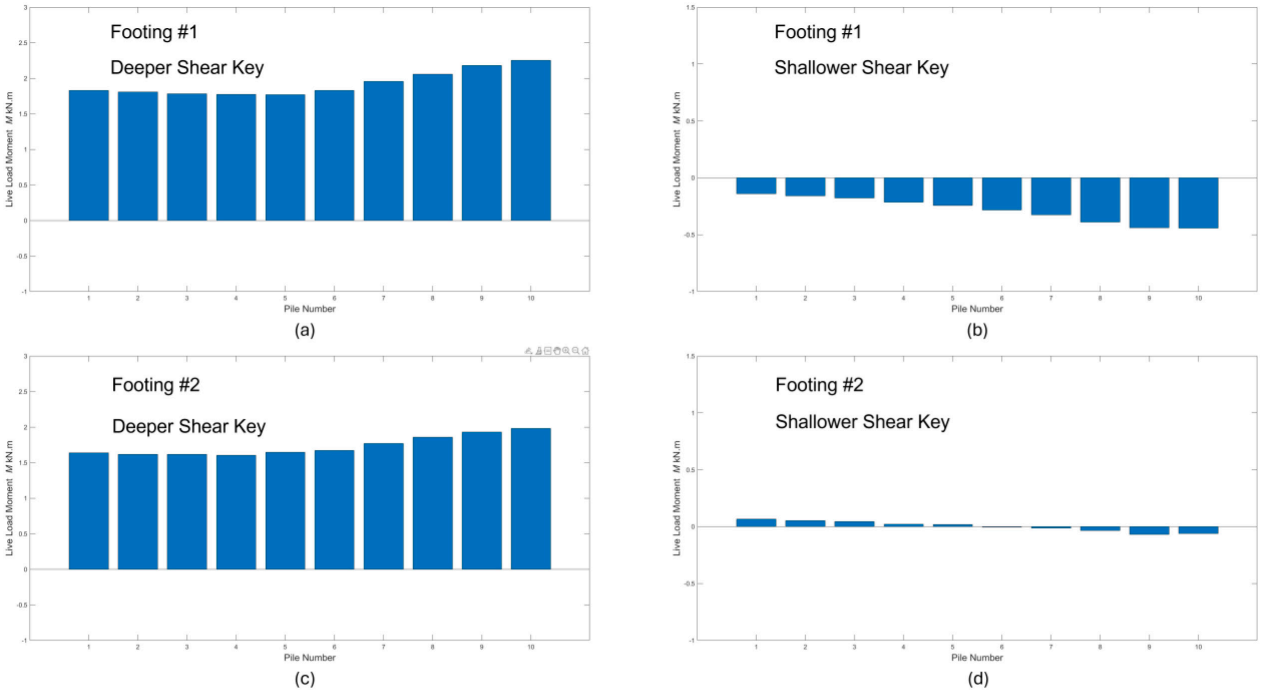

Figure 4.6 Live Load Moment Distributions for Type A Structure With Floating Piles Embedded in NC Clay: (a) Pile Group Under Footing #1 With Deeper Shear Key; (b) Pile Group Under Footing #1 With Shallower Shear Key; (c) Pile Group Under Footing #2 With Deeper Shear Key; (d) Pile Group Under Footing #2 With Shallower Shear Key.

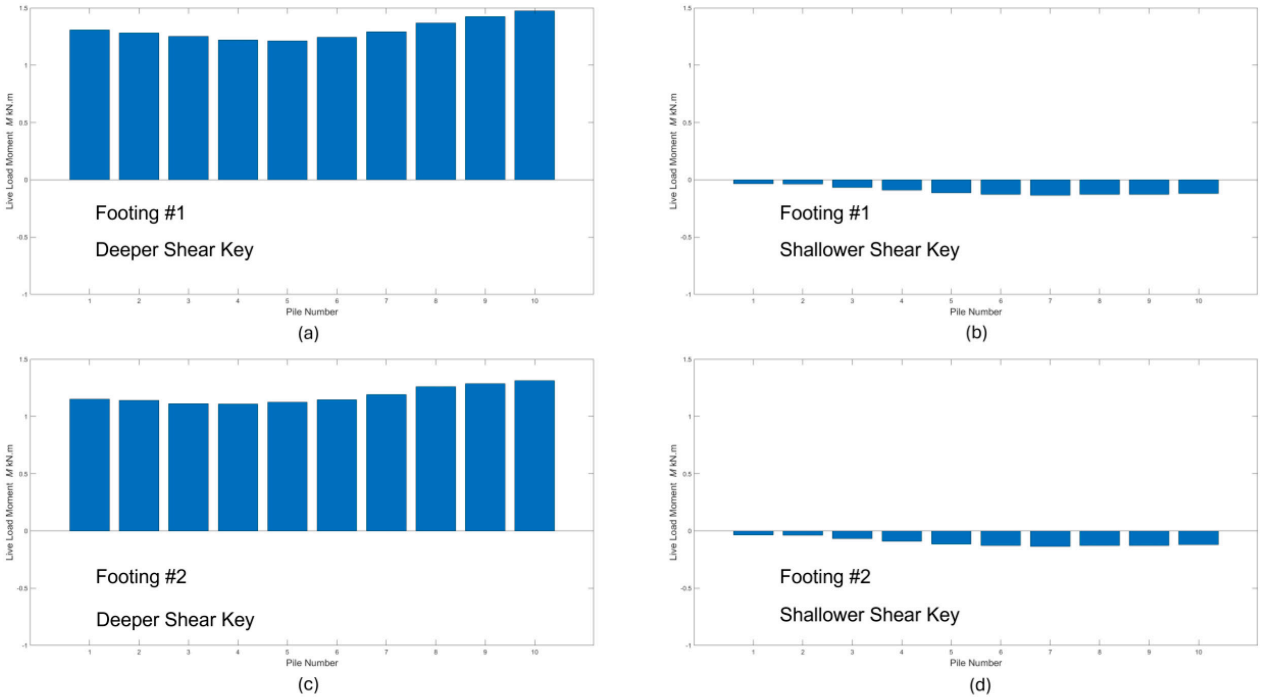

Figure 4.7 Live Load Moment Distributions for Type B Structure With Floating Piles Embedded in NC Clay: (a) Pile Group Under Footing #1 With Deeper Shear Key; (b) Pile Group Under Footing #1 With Shallower Shear Key; (c) Pile Group Under Footing #2 With Deeper Shear Key; (d) Pile Group Under Footing #2 With Shallower Shear Key.

TABLE 4.4
Cap Contribution Analysis: Cap Base Resistance and Pile Resistance Before and After Truck Loading.

Type of Structure	Shear Key Depth	Footing	Cap Base Resistance/ Pile Group Resistance	Before Placing the Truck (kN)	After Placing the Truck (kN)	Live Load Contribution (kN)
Type A	Shallower	Footing #1	Cap base resistance	1326.5 (298.2 kips)	1346.6 (302.7 kips)	20.1 (4.5 kips)
			Pile resistance	1854.1 (416.8 kips)	1988.9 (447.1 kips)	134.8 (30.3 kips)
		Footing #2	Cap base resistance	1375.4 (309.2 kips)	1389.4 (312.3 kips)	17 (3.8 kips)
			Pile resistance	1856.5 (417.4 kips)	1978.6 (444.8 kips)	122.1 (27.4 kips)
	Deeper	Footing #1	Cap base resistance	1141.3 (256.6 kips)	1157.6 (260.2 kips)	16 (3.6 kips)
			Pile resistance	1627.7 (365.9 kips)	1719.7 (386.6 kips)	92 (20.7 kips)
		Footing #2	Cap base resistance	1156.3 (259.9 kips)	1171.4 (263.3 kips)	14.9 (3.3 kips)
			Pile resistance	1673.7 (376.3 kips)	1770.7 (398.1 kips)	97 (21.8 kips)
Type B (6 ft high stem wall)	Shallower	Footing #1	Cap base resistance	1376.5 (309.4 kips)	1392.9 (313.1 kips)	16.4 (3.7 kips)
			Pile resistance	1828.0 (411.0 kips)	1971.8 (443.3 kips)	143.8 (32.3 kips)
		Footing #2	Cap base resistance	1373.4 (308.8 kips)	1387.2 (311.9 kips)	13.8 (3.1 kips)
			Pile resistance	1828.6 (411.1 kips)	1963.7 (441.5 kips)	135.1 (30.4 kips)
	Deeper	Footing #1	Cap base resistance	1233.6 (277.3 kips)	1244.2 (279.7 kips)	10.6 (2.4 kips)
			Pile resistance	1776.0 (399.3 kips)	1890.6 (425.0 kips)	114.6 (25.8 kips)
		Footing #2	Cap base resistance	1367.4 (307.4 kips)	1381.1 (310.5 kips)	13.7 (3.1 kips)
			Pile resistance	1779.1 (400.0 kips)	1895.0 (426.0 kips)	115.9 (26.1 kips)

The simulations involved in this section are all for a floating pile scenario. In the single-truck scenario, the truck is positioned near one side; in the two-truck scenario, the trucks are symmetrically arranged about the road's centerline. Under symmetric loading, the live load on pile 1 should match that on pile 10, pile 2 that on pile 9, and so on. Figure 4.8 shows the plan view of the structure and pile system for the multiple-truck scenario.

Figure 4.9 and Figure 4.10 compare the live load and moment distributions, respectively, for the single- and two-truck cases. To validate the load superposition principle, Figure 4.11 demonstrates that the live load distribution for the case with the two trucks is equivalent to the sum of the live load distributions from two symmetric single-truck cases. For example, adding the loads from pile 1 and pile 10 in the single-truck scenario yields the composite distribution observed in the two-truck case. The live load distribution generated this way is presented in Figure 4.11a. Figure 4.11b shows the live-load distribution generated from multiple truck simulation. We can see the similarity between these two figures. Figure 4.11 only presents the live load carried by the pile group supporting Footing #1. However, this is sufficient, because the results for Footing #2 show the same trend and confirm the same conclusion. This confirmation—that multi-truck loading can be accurately represented as a superposition of single-truck effects—provides an important basis for developing simplified design guidelines. It is important to understand why this is possible: the magnitude of the truck loads does not impose significant inelastic deformation in the soil supporting the three-sided structure.

4.4 Truck Position Effect

The truck position effect was analyzed for the Type A structure. Two scenarios were considered: Case No. 6, with a single truck placed close to one side of the roadway, and Case No. 10, with a single truck placed along the roadway centerline. The two positions and the corresponding pile layout are illustrated in Figure 4.12.

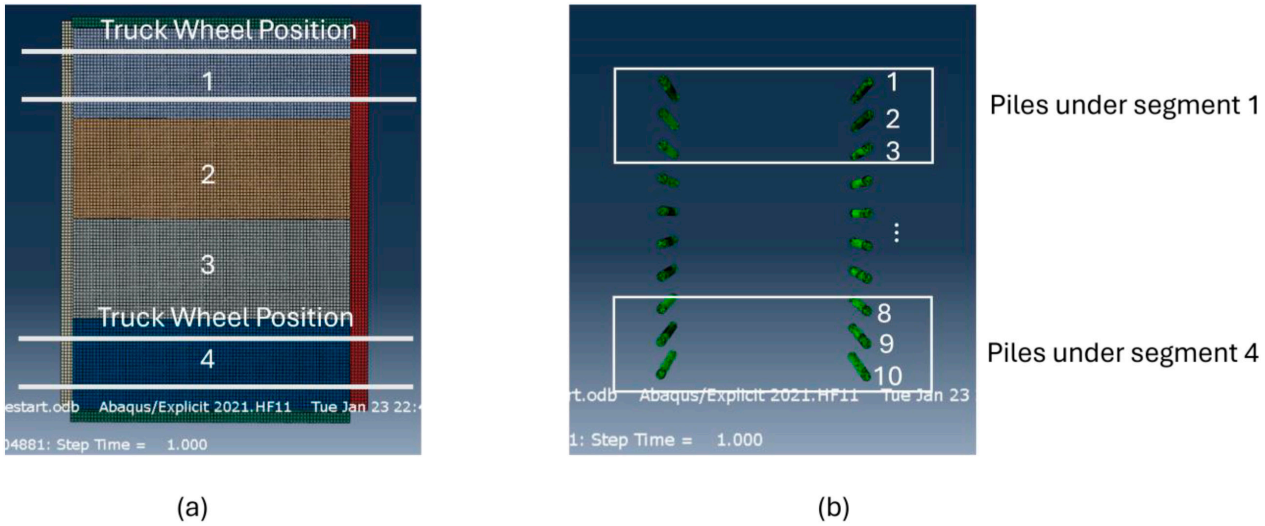

Figure 4.8 Plan View of the Three-Sided Structure and the Piles Supporting the Structure Under Multiple Truck Loading: (a) the Three-Sided Structure With Projected Truck Wheel Position; (b) the Piles Supporting the Three-Sided Structure Labeled With Numbers.

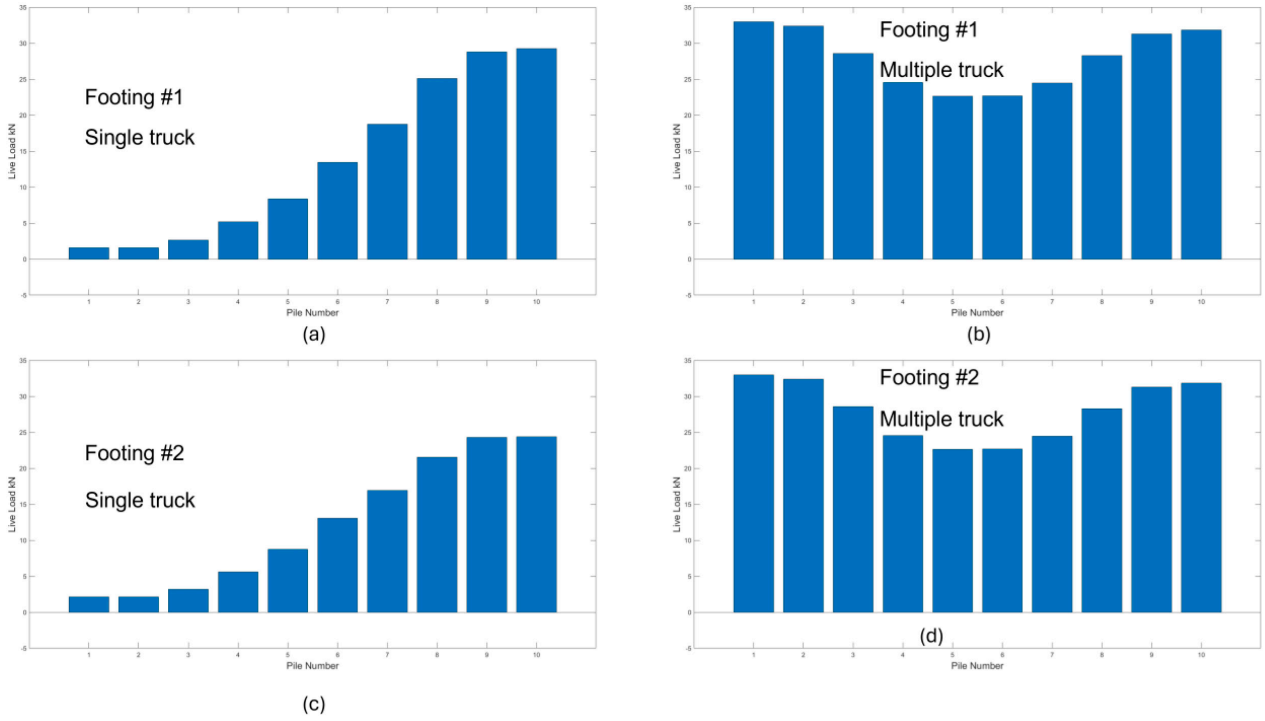

Figure 4.9 Comparison of Live Load Distributions for Single-Truck and Two-Truck Scenarios in Type A Structure.

For the side truck scenario (Case No. 6), the piles directly beneath the loaded segment carried the majority of the live load. The three piles closest to the truck carried about 20% of the total live load, while the three piles farthest from the truck carried less than 2%. The maximum live load on a single pile reached approximately 28 kN (6.3 kips). When the truck was placed along the centerline (Case #10), the load distribution became more uniform. Each pile carried about 7–12% of the live load, and even piles located away from the truck contributed around 10 kN (2.25 kips). The live load distributions for both positions are compared in Figure 4.13.

The live load moment increments were small for both truck positions. For the center truck case, the total moment increment was approximately -1.8 kN·m (-1.33 kips·ft) for Footing #1 and 0.4 kN·m (0.3 kips·ft) for Footing #2, compared to -5.5 kN·m (-4.05 kips·ft) and 0.45 kN·m (0.33 kips·ft) for the side truck case. The moment distribution comparison is shown in Figure 4.14. We can see that the impact of the position of the

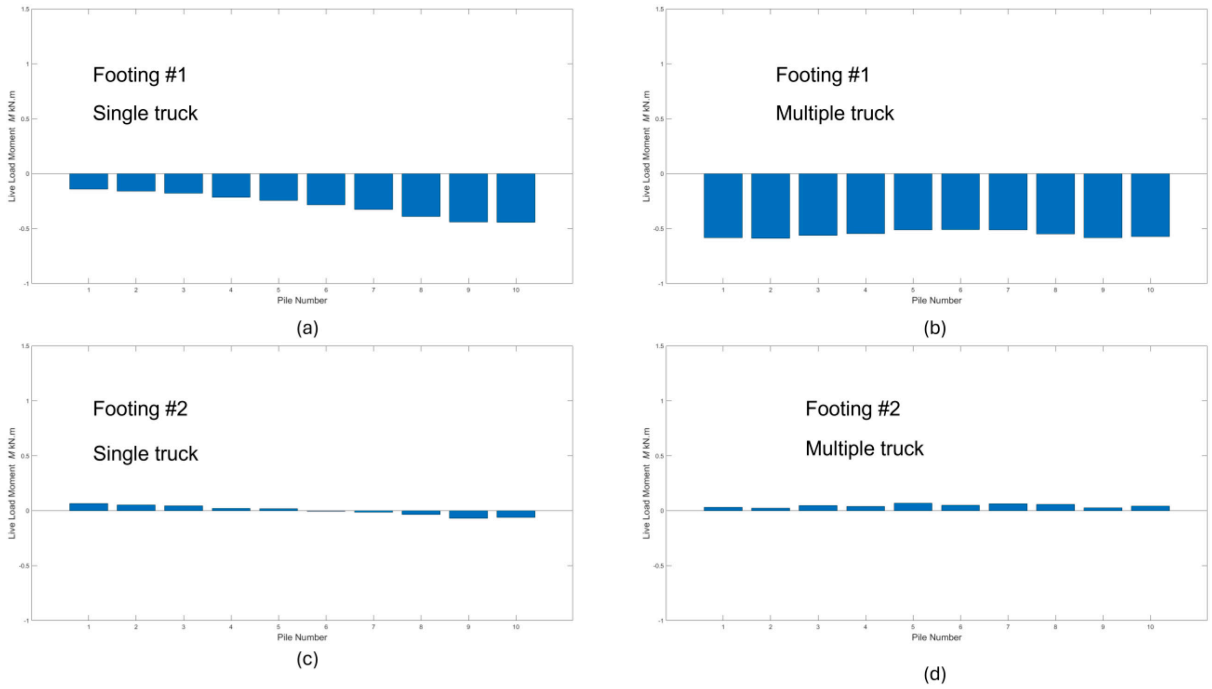

Figure 4.10 Comparison of Live Load Moment Distributions for Single-Truck and Two-Truck Scenarios in Type A Structure.

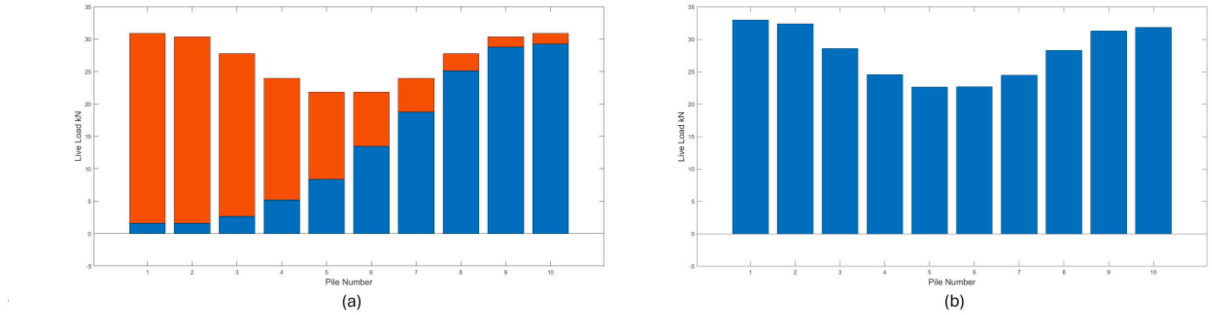

Figure 4.11 Validation of Load Summation Principle: (a) Composite Live Load Distribution From Symmetric Single-Truck Cases; (b) Directly Simulated Live Load Distribution for Two Trucks.

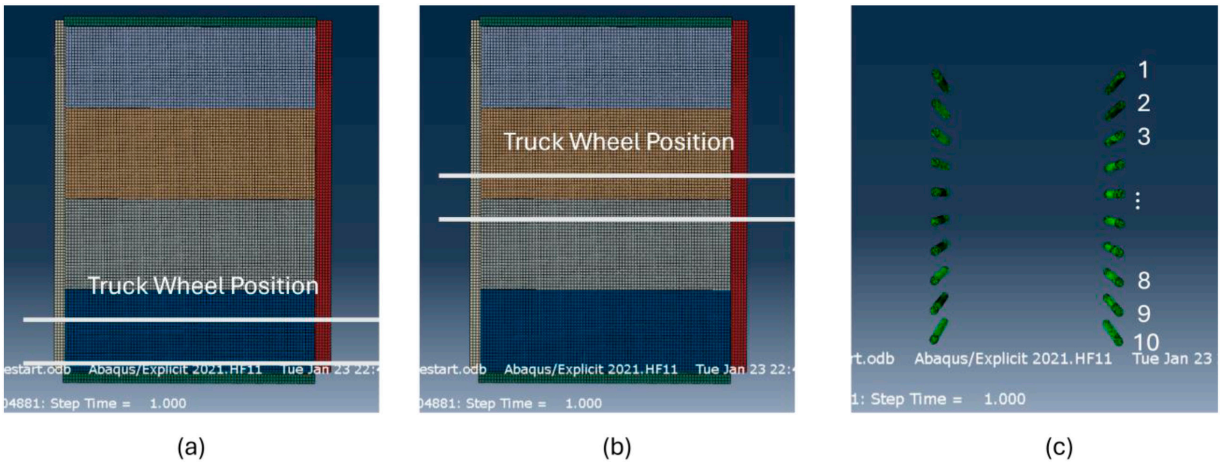

Figure 4.12 Truck Position for Case #6 and Case #10: (a) the Relative Position of the Truck for Case #6, (b) the Truck Wheel Position for Case #10, and (c) the Pile Group Layout.

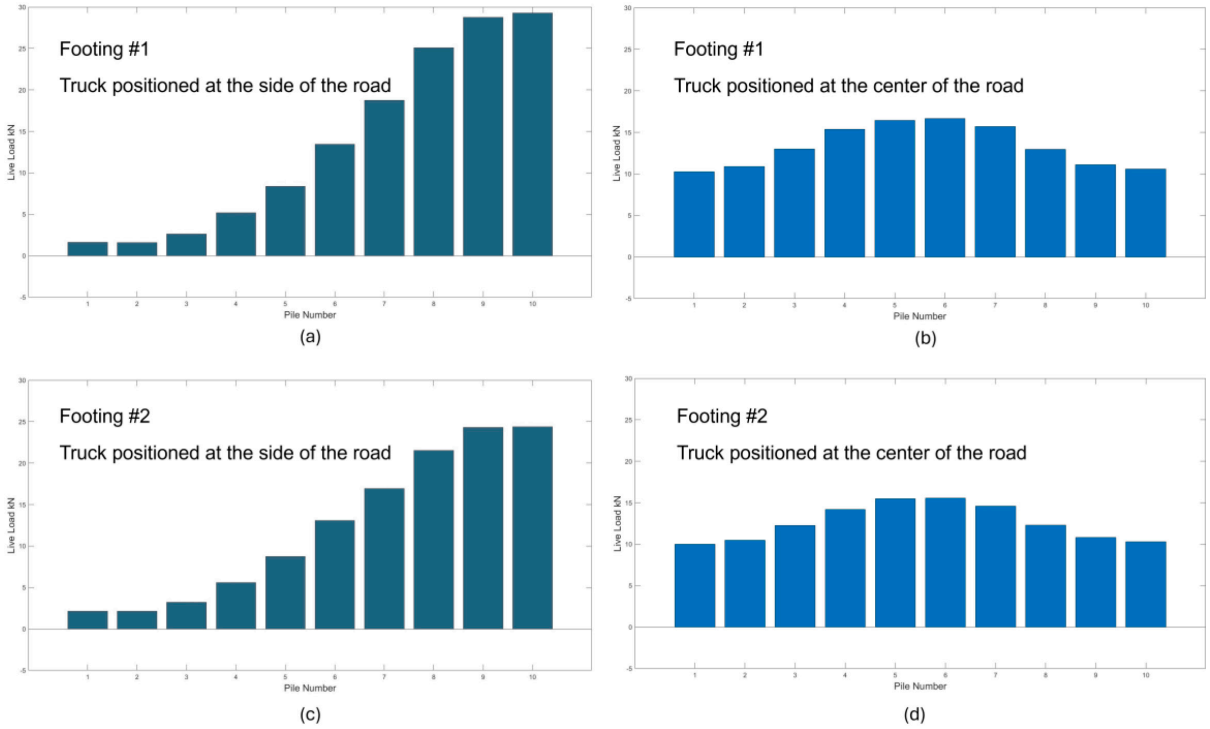

Figure 4.13 Comparison of Live Load Distribution Between the Two Scenarios With the Truck Positioned at Different Locations: (a) Truck Placed at the Side of the Road; (b) Truck Placed at the Center of the Road.

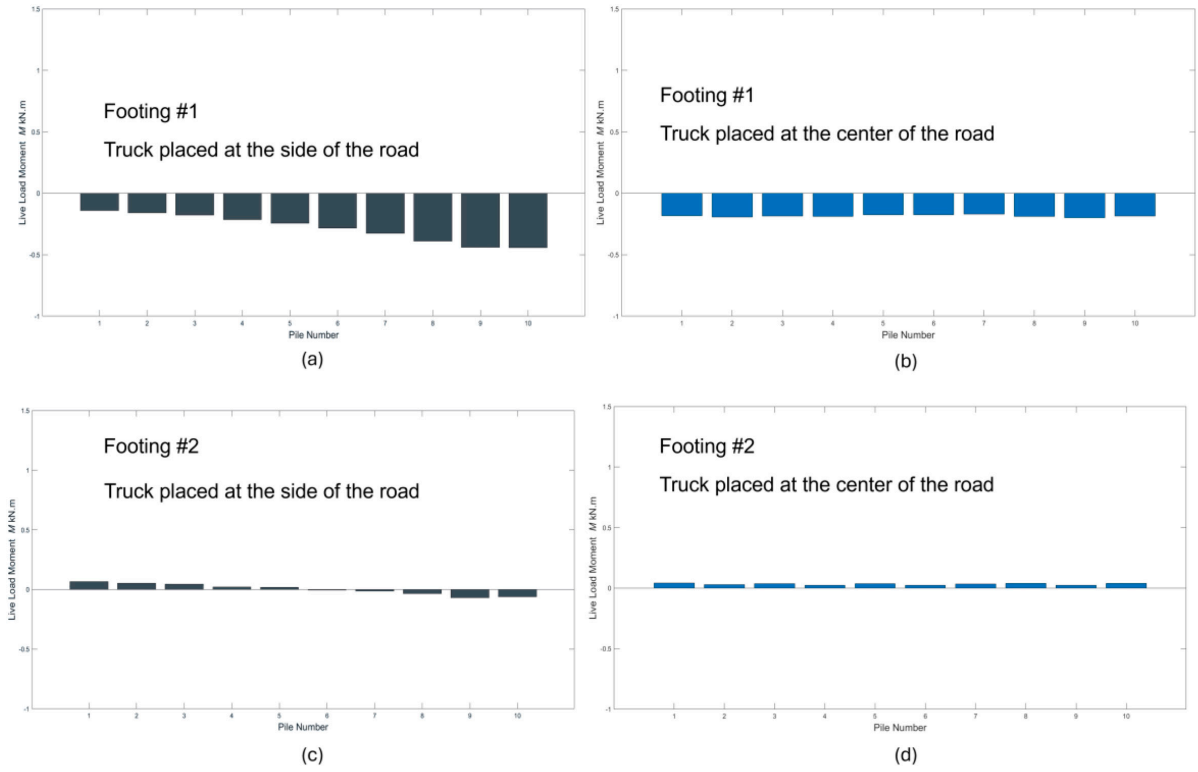

Figure 4.14 Live Load Moment Comparison of Scenarios Where the Truck is Placed at the Side of the Road or at the Center of the Road: (a) Live Load Moment Distribution for Footing #1 for Side Road Scenario; (b) Live Load Moment Distribution for Footing #1 for Center Truck Scenario; (c) Live Load Moment Distribution for Footing #2 for Side Truck Scenario, and (d) Live Load Moment Distribution for Footing #2 for Center Truck Scenario.

truck shows the same trend as it is for live load distribution, with the center truck scenario showing more uniform distribution. However, no matter where the truck was placed, the live load moment is always small enough to be negligible.

4.5 Segment Width Impact

The effect of segment width on live load transfer was evaluated by comparing a three-sided structure with a reduced segment width equal to half of the reference value against the baseline Type A structure with a deep keyway, as discussed in Chapter 4.1. The pile group configuration, soil profile, and applied loads were kept identical between the two models, so the dead load applied to the piles is identical between the two models. In this section, only the live load distribution is presented.

The live load distributions for the two section widths are compared in Figure 4.15. The figure consists of four subplots arranged in two rows and two columns: Figure 4.15a and Figure 4.15b show the live load distributions for Footing #1 in the baseline and reduced-width structures, respectively; Figure 4.15c and Figure 4.15d show the corresponding results for Footing #2. The distribution patterns remain very similar between the two cases. For both footings, piles located directly beneath the loaded segment carry the largest live load increments, ranging from -5–30 kN (-1–7 kips) per pile, corresponding to less than 19% of their respective dead loads. The total live load transferred to the pile groups and the relative distribution among individual piles remain essentially unchanged.

The moment distributions are presented in Figure 4.16, which follows the same subplot layout. Figure 4.16a and Figure 4.16b correspond to Footing #1 for the baseline and reduced-width structures, respectively, while Figure 4.16c and Figure 4.16d show the results for Footing #2. The total live load moment increments are approximately 16.4 kN·m (12.1 kips·ft) for Footing #1 and 17.8 kN·m (13.1 kips·ft) for Footing #2 in the reduced-width structure, which are nearly identical to the baseline case. The comparison demonstrates that segment width reduction has only a minor influence on the moment distribution in both footings.

Overall, these results indicate that segment width has a limited effect on both load and moment distribution in the pile groups. The most critical piles remain those directly beneath the loaded segment, and the magnitude of the maximum total load applied to an individual pile is well below the design capacity of the piles.

4.6 Stem Wall Height Impact

The influence of stem wall height was evaluated by comparing structures with stem wall heights of 0 ft (baseline Type A), 3 ft (0.91 m), and 6 ft (1.83 m). All analyses were performed with a deep shear key, and all other parameters were kept constant.

The live load distributions for the three stem wall heights are compared in Figure 4.17, which shows results for Footing #1. The figure consists of three subplots arranged in a single row. Figure 4.17a corresponds to the 0 ft stem wall structure, Figure 4.17b shows the 3 ft (0.91 m) stem wall case, and Figure 4.17c presents the 6 ft (1.83 m) stem wall structure.

For the 0 ft structure, Figure 4.17a shows a highly non-uniform distribution: piles near the loaded edge (e.g., #8–#10) carry the greatest live-load increments (approximately 27–30 kN or 6–7 kips), while piles on the opposite side carry nearly zero, slightly negative load increments. For the 3 ft stem wall, Figure 4.17b shows a much flatter profile across pile numbers.

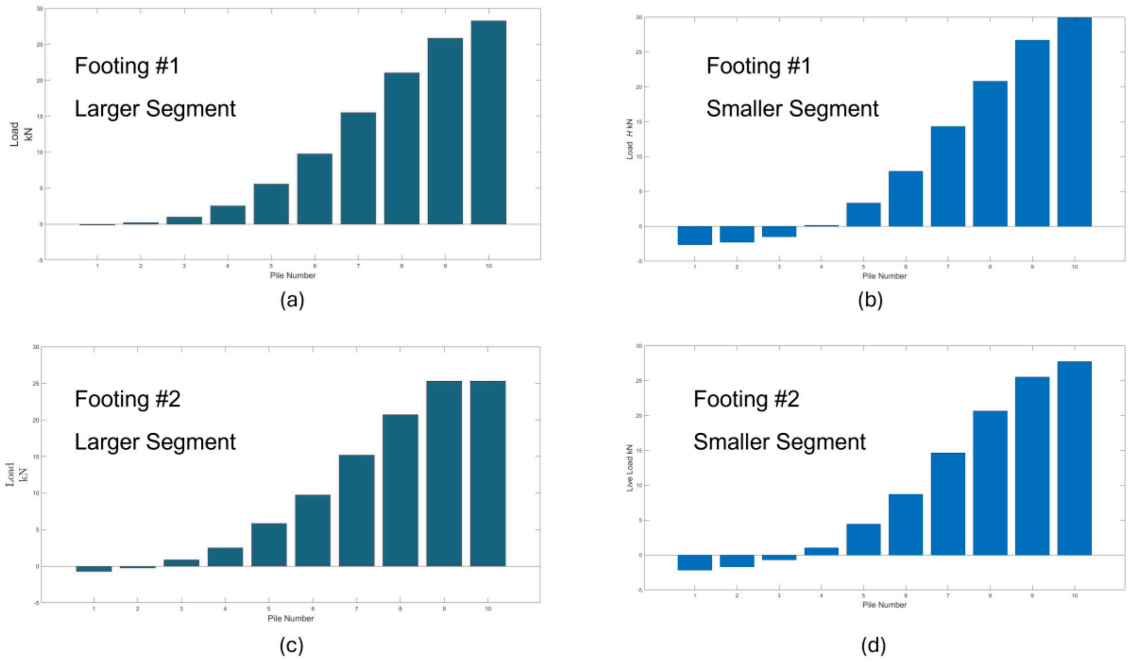

Figure 4.15 Segment Width Impact on Live Load Distributions in the Pile Group: (a) Live Load Distribution for Pile Group Under Footing #1 for the Baseline Scenario; (b) Live Load Distribution for Pile Group Under Footing #1 for Smaller Segment Width Scenario; (c) Live Load Distribution for Pile Group Under Footing #2 for Baseline Scenario, and (d) Live Load Distribution for Pile Group Under Footing #2 for Smaller Segment Width Scenario.

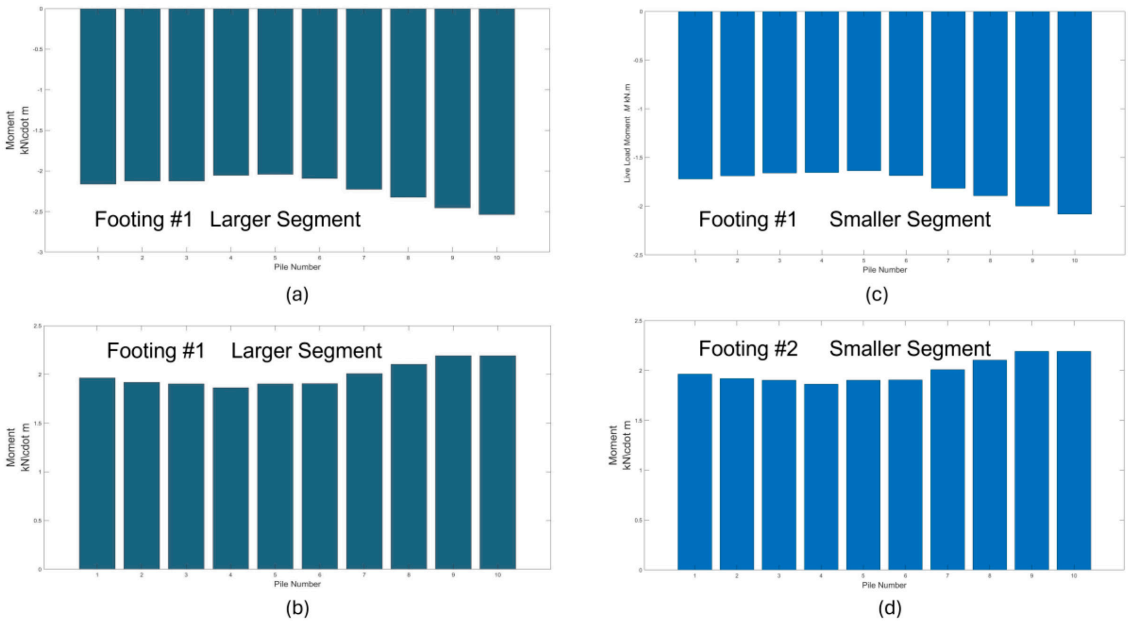

Figure 4.16 Segment Width Impact on Live Load Moment Distributions in the Pile Group (a) Live Load Moment Distribution for Pile Group Under Footing #1 for the Baseline Scenario; (b) Live Load Moment Distributions for Pile Group Under Footing #1 for Smaller Segment Width Scenario; (c) Live Load Moment Distributions for Pile Group Under Footing #2 for Baseline Scenario, and (d) Live Load Moment Distributions for Pile Group Under Footing #2 for Smaller Segment Width Scenario.

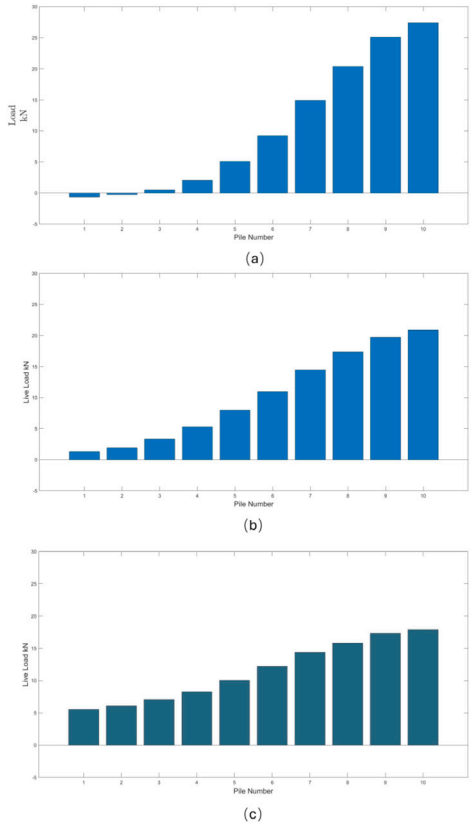

Figure 4.17 Live Load Distribution for Footing #1: (a) Live Load Distribution for Scenario With Stem Wall Heights of 0 ft; (b) Live Load Distribution for Scenario With Stem Wall Heights of 3 ft (0.91 m), and (c) Live Load Distribution for Scenario With Stem Wall Heights of 6 ft (1.83 m).

The maximum live load carried by an individual pile is about 21 kN (4.72 kips), and the average live load is 10 kN (2.25 kips) for both footings (approximately 6–7% of the dead load). Relative to 0 ft, peaks are reduced, and piles further from the truck pick up more load, though the local maximum remains near the loaded edge. For the 6 ft (1.83 m) stem wall, Figure 4.17c shows that the distribution is further evened out. However, the significance of the changes is different. The change from 0 ft to 3 ft (0.91 m) is pronounced, whereas the change from 3 ft (0.91 m) to 6 ft (1.83 m) is relatively small.

Figure 4.18 summarizes the maximum live load carried by an individual pile as a function of stem wall height for Footing #1, illustrating the same trend.

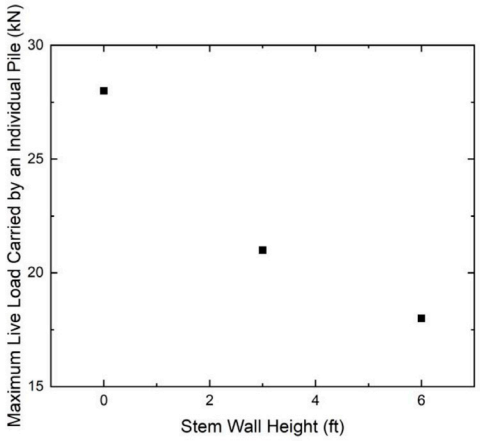

Figure 4.18 Maximum Live Load Carried by an Individual Pile vs. Stem Wall Height for Footing #1. The Footing Numbers are Shown in Figure 4.2.

The moment for the 3-ft (0.91 m) stem wall falls between those for the 0 ft and 6 ft (1.83 m) cases. Since shear key depth governs the overall moment behavior more strongly than stem wall height under the current loading configuration, detailed results will not be presented in this section.

4.7 Vertically Non-Uniform Soil Profile Impact

The influence of a vertically non-uniform soil profile on live load transfer was evaluated for the Type A structure with the shallow shear key configuration and 20-m-long piles (66 ft). In this analysis, an upper sublayer of the clay layer with a thickness equal to five times the pile diameter B was modeled as slightly over-consolidated (OCR = 3), while the remaining profile consisted of normally consolidated clay, consistent with the baseline configuration used in previous simulations, as shown in Figure 3.2.

The simulation results indicate that the presence of the slightly over-consolidated clay has only a minor effect on the overall live load transfer to the piles. For the piles supporting Footing #1, the average live load increases from 11.45 kN (2.57 kips) in the uniformly normally consolidated case to 13.45 kN (3.02 kips) in the non-uniform case, while for piles supporting Footing #2, the corresponding change is from 12.2 kN (2.74 kips) to 12.35 kN (2.78 kips). The maximum live load for Footing #1 reaches approximately 32 kN (7.19 kips), which is only slightly higher than in the uniform condition. These variations suggest that the difference in load transfer behavior between the two soil profiles is negligible.

The overall pattern of live load distribution within the pile group remains consistent with that observed in the uniform soil case. Piles 8, 9, and 10 carry most of the live load, while Pile 1, located farthest from the truck load, contributes almost no load. This confirms that the introduction of a slightly over-consolidated clay layer near the surface does not alter the fundamental mechanism of load sharing among piles (see Figure 4.19). The live load moments are very small in both configurations and can be neglected in the overall comparison.

In summary, introducing a slightly over-consolidated layer into the upper clay region produces only a minor change in the magnitude of live load transfer and no noticeable effect on the load distribution pattern across the pile group.

4.8 Earth Cover Depth Effect

The effect of earth cover depth on the live load transferred to the piles was examined for the Type A structure with the deep shear key configuration. Three cover depths—1 ft, 2 ft, and 4 ft—were analyzed to evaluate how the increased thickness of the soil layer influences the magnitude of live load transmitted from the traffic surface to the substructure.

The results indicate that the overall magnitude of the live load transferred to the piles decreases as the earth cover becomes thicker. This reduction occurs because the additional soil cover helps distribute and absorb the applied load before it reaches the structure. For the 1-ft (0.31-m) cover, the maximum live load acting on Footing #1 reaches about 28 kN. Increasing the cover to 2 ft (0.61 m) results in a slight reduction, with the maximum load decreasing to approximately 23 kN (5.17 kips). When the cover is increased to 4 ft (1.22 m), the maximum live load further decreases to about 20 kN (4.50 kips). The pile group supporting Footing #2 shows a similar trend with slightly different values of maximum live load. The maximum load decreases to

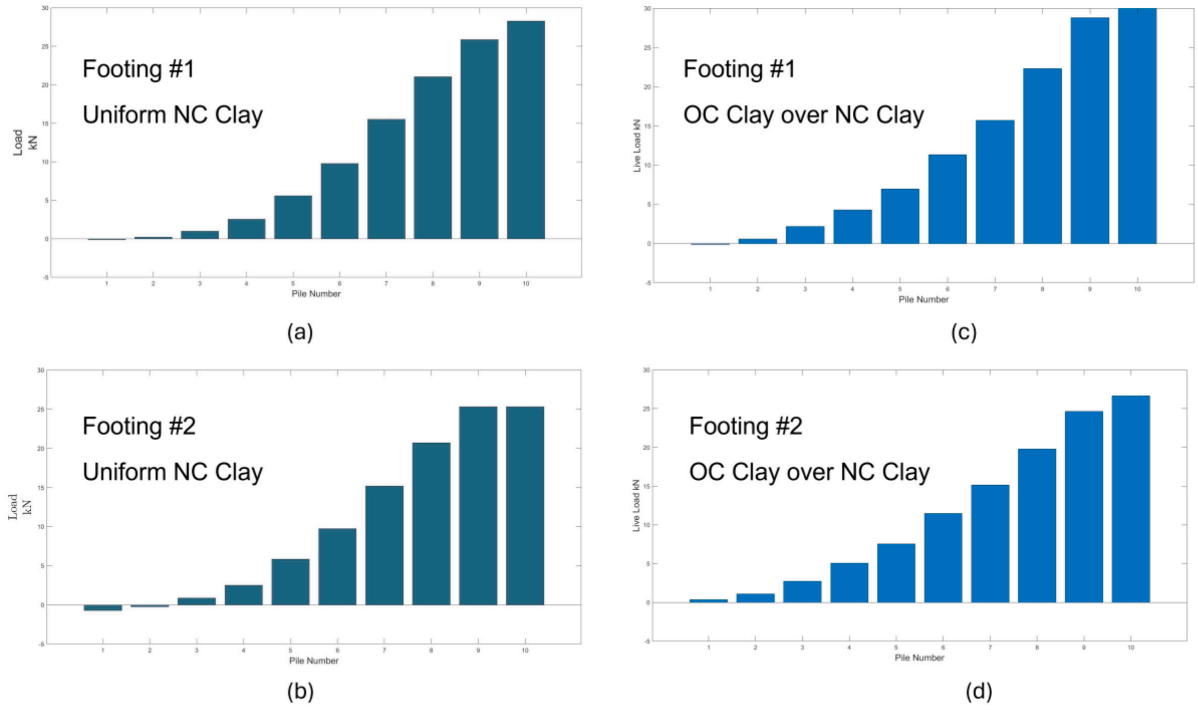

Figure 4.19 Live Load Distribution Comparison for Type A Structure Under Non-Uniform and Uniform Soil Profiles.

approximately 25 kN (5.62 kips) when the earth cover depth increases to 2 ft (0.61 m), and the maximum load decreases to 22 kN (4.95 kips) when the earth cover increases to 4 ft (1.22 m). This trend shows that the change from 1 ft (0.31 m) to 2 ft (0.61 m) produces only a minor reduction, whereas the 4-ft case introduces a more significant attenuation of live load transfer. Figure 4.20 shows the live load distribution within the pile group below Footing #1 for these three different scenarios.

Although the load magnitudes vary with cover depth, the overall distribution pattern within the pile group remains essentially the same. The piles under the truck—particularly piles 8, 9, and 10—consistently carry most of the live load, while piles far from the truck, such as pile 1, carry very little. This indicates that increasing the earth cover reduces the overall live load magnitude, without altering the live load distribution pattern among piles.

The live load moments exhibit a similar trend; however, the magnitude of the moment change due to varying earth cover depth is small compared with the effect of the shear key depth

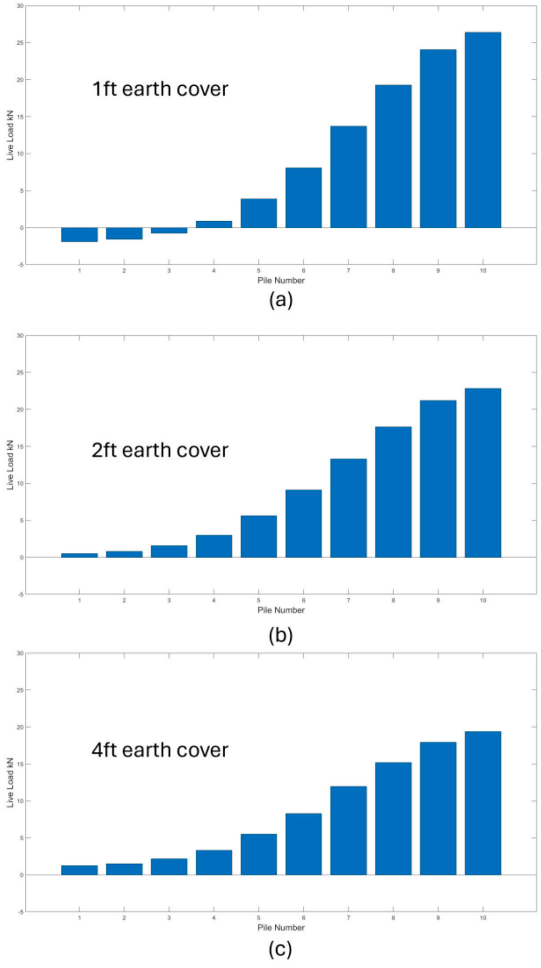

Figure 4.20 Live Load Distribution of the Pile Group Below Footing #1 for Three Different Scenarios: (a) Earth Cover Depth of 1 ft (0.31 m), (b) Earth Cover Depth of 2 ft (0.61 m), and (c) Earth Cover Depth of 4 ft (1.22 m).

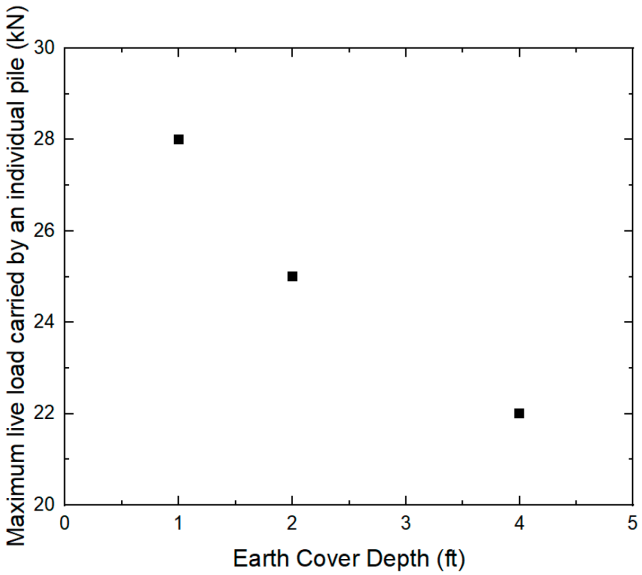

Figure 4.21 Maximum Live Load Carried by the Individual Piles for Three Different Scenarios With Different Earth Cover Depth.

and can be neglected in the overall evaluation. Therefore, the discussion here focuses primarily on the live load variations.

In summary, thicker earth cover reduces the live load transmitted to the piles while maintaining a consistent distribution pattern. The difference between 1 ft (0.31 m) and 2 ft (0.61 m) is modest, but the reduction becomes more pronounced when the cover increases to 4 ft (1.22 m).

5. DESIGN GUIDELINES FOR THREE-SIDED STRUCTURES

5.1 Lessons Learned

The results of the parametric analyses allow several general observations that can be the basis for preliminary guidelines for design.

5.1.1 Truck Position Effect

The most critical live-load condition occurs when an HL-93 truck is positioned near the roadway edge. In such cases, the three piles directly beneath the loaded segment carry approximately 18–22% of the total live load each, while the piles farthest from the truck contribute less than 5%. When the truck is centered on the roadway, the load distribution becomes much more uniform, with each pile carrying between 7% and 12% of the total live load. Therefore, edge-loading conditions should generally be treated as the governing scenario for live-load design of pile-supported three-sided structures.

5.1.2 Stem Wall Stiffness

The analyses considered stem-wall heights of 0 ft, 3 ft (0.91 m), and 6 ft (1.83 m), which are commonly used in practice. Under the modeled conditions, increasing the stem-wall height leads

to a more uniform live-load distribution among piles: the peak live load on an individual pile decreases by about 25% when the height increases from 0 ft to 3 ft (0.91 m), and by about 35% when it increases from 0 ft to 6 ft (1.83 m); the improvement from 3 ft to 6 ft is modest, indicating diminishing marginal benefit beyond 3 ft (0.91 m). Within the common 0–6 ft (0–1.83 m) range, the relationship is non-linear. A height near 3 ft (0.91 m) generally offers a good balance between improved load uniformity and constructability; the final choice should also consider structure weight, overall geometry, and construction feasibility under project-specific conditions.

5.1.3 Earth Cover Depth

Earth-cover depths of 1 ft (0.31 m), 2 ft (0.61 m), and 4 ft (1.22 m) were analyzed, representing typical field conditions. Increasing the cover reduced the maximum live load on an individual pile by about 10% when earth cover increased from 1 ft to 2 ft, and by about 20% when it increased from 1 ft to 4 ft. The overall distribution pattern remained similar—piles directly beneath the loaded area continued to carry most of the live load, while the farthest piles carried little or none. The results suggest that the soil above the structure absorbs part of the live load but does not fundamentally change its distribution. In design, earth cover should therefore be considered when estimating live-load magnitude, but not to redistribute load among piles.

5.1.4 Shear Key Configuration

The depth of the shear key has negligible influence on the vertical load distribution among the piles. While a deeper key provides additional rotational restraint, the shallow key behaves effectively as a pinned connection. In both configurations, the live-load moments transmitted to individual piles remain very small (less than 5 kN·m or 3.7 kips·ft) and can be considered negligible for design purposes.

5.1.5 Pile Cap Repeated Contribution

Simulation results indicate that the direct bearing of the pile cap and the surrounding soil beneath the footing accounts for a relatively small portion of the total live load transmitted to the base of the foundation. For example, under the modeled conditions, the pile cap directly resists approximately 10% of the total live load. Designers should recognize its presence as a secondary load-sharing mechanism that enhances the overall system stiffness.

5.1.6 Segment Width

Variation of the segment width from 10 ft (3.05 m) to 5 ft (1.52 m) resulted in less than 2% change in the maximum pile reaction, suggesting that the live-load distribution is insensitive to this parameter. Segment width within this range can therefore be selected based on construction and manufacturing considerations rather than structural performance.

5.1.7 Soil Profile Effects

Introducing a moderately over-consolidated surface clay layer above the normally consolidated clay slightly increases foundation stiffness but does not significantly affect the live-load distribution pattern. The same design approach may be applied to both normally consolidated and moderately over-consolidated clays, as the pile-group behavior remains largely similar.

5.1.8 Multiple-Truck Loading and Superposition

The superposition principle approximately holds for well-designed and adequately stiff pile groups. The combined effects of two side-by-side trucks are nearly equal to the algebraic sum of single-truck cases, with a difference within 5%. Consequently, linear superposition of single-lane loading can be used for preliminary estimation of multi-lane live loads when the pile design is modestly conservative to overconservative.

5.2 Comparison Between Traditional Design and Simulation Results

To evaluate the reliability of the traditional design approach for estimating live-load effects in three-sided structures, the moment-of-inertia method currently used in INDOT practice was first examined.

In this method, the pile cap is treated as a rigid body that transfers all vertical reactions through the piles, and the live load from a truck is represented by a total vertical force P and an overturning moment M = P × e, where e is the horizontal eccentricity of the applied load relative to the pile-group centroid.

Assuming that the pile heads remain in a single plane after deformation, the vertical reaction in each pile can be expressed as a linear function of its position x_i relative to the gravity center of the pile group

$$P_i = \frac{P}{n} + \frac{Mx_i}{\Sigma x_i^2} \tag{1}$$

where n is the number of piles and Σx_i^2 is the geometric "moment of inertia" of the pile layout about the centroidal axis, and M is the moment created by the truck.

This formulation assumes identical axial stiffness among all piles and neglects direct bearing of the pile cap or soil contact beneath it.

Consequently, piles located on the loaded side receive the highest compressive reactions, while those on the far side may experience reduced load or uplift.

Using this idealized assumption and applying the live load symmetrically to both sides of the structure, the maximum live-load increment on a single pile was calculated to be approximately 43 kN (9.6 kips). If a multiple presence factor of 1.2 is considered, then the maximum live load carried by an individual pile is approximately 52 kN (11.7 kips). The live load distribution calculated using this method without a multiple presence factor is shown in Figure 5.1.

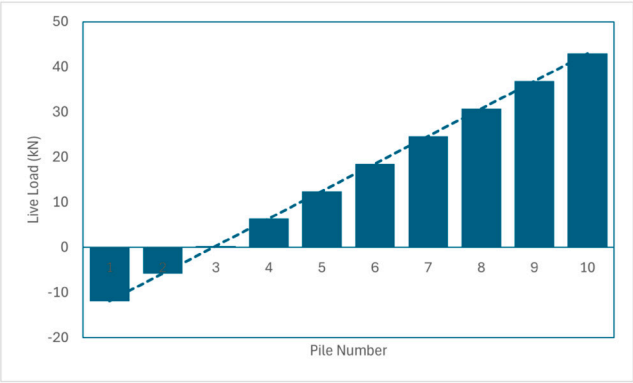

Figure 5.1 Live Load Distribution Calculated Using Traditional Moment of Inertia Method With Equally Distributed Live Load Between Footing #1 and Footing #2, Ignoring the Load Absorption of the Materials Above the Piles.

By comparison, the finite-element simulation of the same configuration (Type A structure with a shallow shear key) predicted a peak pile load of only 28 to 30 kN (6.3–6.7 kips).

The difference—about 50%—illustrates that the traditional linear distribution method tends to overestimate pile reactions when the load-sharing effects of the pile cap and adjacent soil are ignored.

The initial comparison revealed that the simplified linear distribution method substantially overestimates pile reactions because it neglects the load-sharing contribution of the pile cap and the soil surrounding the structure.

To improve the consistency of the comparison and better represent the observed structural behavior, the same Type A shallow-key configuration was subsequently re-evaluated by incorporating the live-load distribution pattern obtained from the numerical simulations into the moment-of-inertia framework.

In this refined calculation, the design truck was positioned near the outside lane, corresponding to the governing case identified in the numerical analyses.

The refined calculation results are shown in Figure 5.2. In this refined calculation, the total live load of 134 kN (30.1 kips) was distributed linearly among ten piles according to their horizontal coordinates, yielding a peak reaction of 37 kN (8.3 kips) on the loaded side and 33 kN (7.4 kips) on the opposite side.

The refined comparison shows that, when consistent assumptions are applied, the traditional moment-of-inertia method predicts maximum pile reactions that are about 10–15% greater than those obtained from detailed simulations.

This level of conservatism is considered reasonable for preliminary design and provides a clear upper bound on expected pile demand.

Accordingly, the moment-of-inertia method can continue to serve as a practical screening tool for INDOT designers, while detailed finite-element analyses are recommended only for nonstandard geometries, higher importance structures, or configurations exhibiting significant stiffness variation between substructures.

5.3 Design Recommendations

The results of the parametric analyses and the comparative evaluation between traditional and simulation-based approaches provide several clear directions for the design of three-sided structures supported on deep foundations.

The analyses confirm that the most critical live-load effects occur when the design truck is positioned near the roadway edge. This loading configuration should therefore govern the evaluation of live-load distribution and the design of individual pile reactions.

The pile cap should be regarded as an active participant in load transfer rather than merely a connection element. Simulation results indicate that direct bearing of the cap and the adjacent soil can resist roughly 10% of the total live load for conditions similar to those considered here. Contributions could be more significant when the cap bears on stronger material. The stem wall combined with the footing forms a critical component of the whole supporting system of the structure that helps adjust the live-load distribution.

The live load is also partly dissipated by the soil-structure interaction above the piles, which should be considered during design. Increasing earth cover depth reduces the magnitude of the maximum live load carried by the piles.

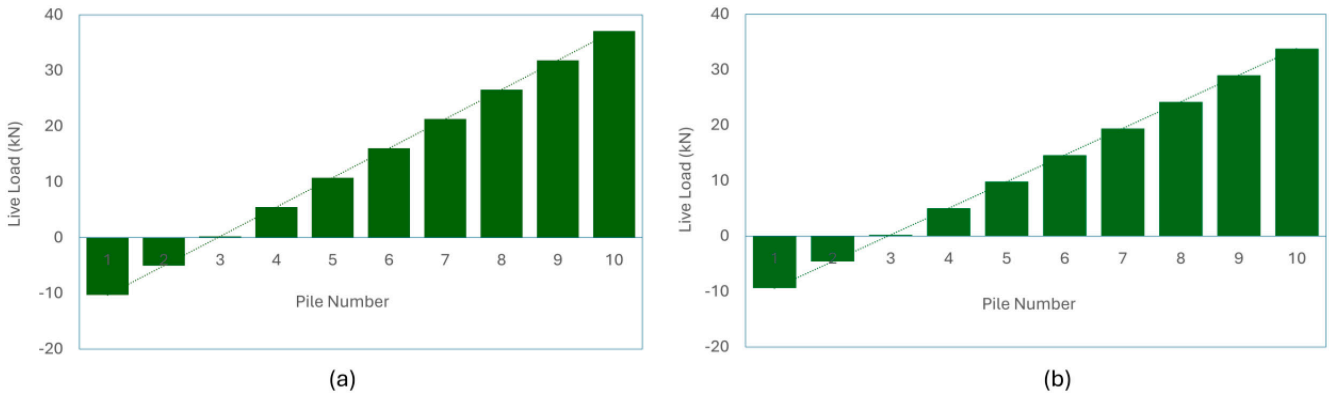

Figure 5.2 The Live Load Distribution Calculated Using the FEA Derived Live Load Carried by the Piles and the Traditional Moment of Inertia Method: (a) for Footing #1 and (b) for Footing #2.

When examined under consistent assumptions, the traditional moment-of-inertia method was found to predict maximum pile reactions about 10% to 15% higher than those from detailed simulations. This moderate conservatism supports its continued use as a practical upper-bound tool for preliminary design and screening-level evaluations. Designers should, however, ensure that the assumed live-load distribution and pile-group geometry in the calculation remain consistent with the actual structural configuration. It should also be noted that the study evaluated only a 12 m (approximately 40 ft) long structure, and the conservatism associated with the method's underlying assumptions may decrease as structural length increases.

For typical INDOT geometries and boundary conditions, the traditional moment-of-inertia method remains suitable for preliminary design and general screening of live-load effects. More refined numerical analyses should be reserved for cases involving asymmetric stiffness, nonstandard geometry, or partial scour exposure. In all cases, design should emphasize serviceability performance—considering differential settlement and rotational compatibility between adjacent footings—and ultimate limit state avoidance, because all simulated live-load effects remain well below the structural capacity of the foundation elements.

6. CONCLUSION

This study investigated load transfer behavior in pile-supported buried three-sided structures through a national survey of DOT engineers and a series of three-dimensional finite element analyses. The survey confirmed that, although these structures are increasingly used where spread footings are not feasible due to scour, weak soils, or site constraints, design approaches for distributing loads to piles remain inconsistent and commonly rely on engineering judgment. To address these issues, finite element analyses were conducted on a representative buried three-sided structure with documented modeling assumptions, and key parameters were varied individually to assess their influence on load sharing among piles.

For the modeled conditions, earth cover depth and stem wall height had the most notable influence on live-load distribution. Increased earth cover and taller stem walls led to more uniform live load distribution among piles, which is preferred for design. Shear key depth did not affect live-load distribution but influenced moment transfer between the structure and foundation system; however, the resulting pile head moments were small enough to be considered negligible. Truck position governed the most critical live-load distribution scenario: when the truck was positioned near the roadside, the piles beneath that section carried approximately 20% of the total live load transferred to the pile group, while the piles farthest from the truck carried almost none. When the truck was centered, live-load distribution became more uniform, and all piles contributed. Changes in segment width and the presence of a slightly over-consolidated clay layer above normally consolidated clay had minimal impact.

Comparison between the finite element results and the traditional moment-of-inertia design approach showed that the traditional method overpredicts live load transferred to piles by roughly 50% when soil and structural contributions are ignored, and by approximately 10–15% when those contributions are considered. As such, the traditional approach may still be suitable for preliminary design, but more realistic numerical analyses are recommended for design-level evaluations that require accurate assessment of load sharing.

The conclusions apply to the structure configuration, soil conditions, and loading scenarios used in this study. Applicability should be evaluated on a project-specific basis, particularly where soil profiles, geometry, construction details, or loading conditions differ from those modeled. Additional field monitoring and further analyses would support refinement of these findings and inform potential adoption into DOT practice.

REFERENCES

American Association of State Highway and Transportation Officials. (2020). *LRFD bridge design specifications* (9th ed.). AASHTO.

ASTM International. (1999). *Standard practice for minimum structural design loading for monolithic or sectional precast concrete water and wastewater structures* (ASTM C890-91[1999]e1). https://doi.org/10.1520/C0890-91R99E01

Awwad, E., Mabsout, M., Sadek, S., & Tarhini, K. (2000). Finite element analysis of concrete box culverts. In R. Fruchter, F. Peña-Mora, & W. M. Kim Roddis (Eds.), *Computing in civil and building engineering* (pp. 1051–1053). American Society of Civil Engineers. https://doi.org/10.1061/40513(279)136

Bennett, R. M., Wood, S. M., Drumm, E. C., & Rainwater, N. R. (2005). Vertical loads on concrete box culverts under high embankments. *Journal of Bridge Engineering*, *10*(6), 643–649. https://doi.org/10.1061/(ASCE)1084-0702(2005)10:6(643)

Chakraborty, T., Salgado, R., & Loukidis, D. (2013). A two-surface plasticity model for clay. *Computers and Geotechnics*, *49*, 170–190. https://doi.org/10.1016/j.compgeo.2012.10.011

Dasgupta, A., & Sengupta, B. (1991). Large-scale model test on square box culvert backfilled with sand. *Journal of Geotechnical Engineering*, *117*(1), 156–161. https://doi.org/10.1061/(ASCE)0733-9410(1991)117:1(156)

Dassault Systèmes. (2024). *Abaqus* [Computer software].

Garg, A. K., & Abolmaali, A. (2009). Finite-element modeling and analysis of reinforced concrete box culverts. *Journal of Transportation Engineering*, *135*(3), 121–128. https://doi.org/10.1061/(ASCE)0733-947X(2009)135:3(121)

Han, F., Prezzi, M., Salgado, R., Marashi, M., Wells, T., & Zaheer, M. (2020). *Verification of bridge foundation design assumptions and calculations* (Joint Transportation Research Program Publication No. FHWA/IN/JTRP-2020/18). Purdue University. https://doi.org/10.5703/1288284317084

Kadivar, M., Manahiloh, K. N., Kaliakin, V. N., & Shenton, H. W. (2018). Numerical investigation of dynamic load amplification in buried culverts. *Transportation Infrastructure Geotechnology*, *5*(1), 24–41. https://doi.org/10.1007/s40515-017-0045-7

Loukidis, D., & Salgado, R. (2009). Modeling sand response using two-surface plasticity. *Computers and Geotechnics*, *36*(1–2), 166–186. https://doi.org/10.1016/j.compgeo.2008.02.009

Minnesota Department of Transportation. (2013). *LRFD bridge design manual*. https://www.dot.state.mn.us/bridge/lrfd.html

Ozturk, K. F. (2024). Investigation of dynamic responses of three-sided underpass culvert under near-fault and far-fault ground motions considering soil-structure interaction. *Soil Dynamics and Earthquake Engineering*, *177*, 108446. https://doi.org/10.1016/j.soildyn.2023.108446

Pimentel, M., Costa, P., Félix, C., & Figueiras, J. (2009). Behavior of reinforced concrete box culverts under high embankments. *Journal of Structural Engineering*, *135*(4), 366–375. https://doi.org/10.1061/(ASCE)0733-9445(2009)135:4(366)

Poulos, H. G., & Davis, E. H. (1974). *Elastic solutions for soil and rock mechanics*. John Wiley & Sons, Inc.

Poulos, H. G., & Mattes, N. S. (1971). Settlement and load distribution analysis of pile groups. *Australian Geomechanics Journal*, *g1*(1), 18–28.

Ramadan, S. H., & El Naggar, M. H. (2022). Design guidelines for reinforced concrete three-sided culverts. *Tunnelling and Underground Space Technology*, *119*. https://doi.org/10.1016/j.tust.2021.104259

Salgado, R. (2022). *The engineering of foundations, slopes and retaining structures* (2nd ed.). CRC Press. https://doi.org/10.1201/b22079

Wang, S., Feng, Z., Guo, C., Wei, J., & Zhao, R. (2024). Research on the method of identifying vertical earth pressure of hinged prefabricated culvert box culvert on the top slab. *Scientific Reports*, *14*. https://doi.org/10.1038/s41598-024-69893-4

Wang, Y., Lim, J., Salgado, R., Prezzi, M., & Hunter, J. (2022). *Pile stability analysis in soft or loose soils: Guidance on foundation design assumptions with respect to loose or soft soil effects on pile lateral capacity and stability* (Joint Transportation Research Program Publication No. FHWA/IN/JTRP-2022/24). Purdue University. https://doi.org/10.5703/1288284317387

Washington State Department of Transportation. (2015, November 30). *WSDOT precast concrete culvert standards* [Design memorandum]. https://wsdot.wa.gov/Publications/Fulltext/Bridge/Designmemos/07-2015.PDF

Wells, A. C. (2016). *Analytical and experimental investigation of dynamic amplification factor for the load rating of reinforced concrete box culverts* (Master's thesis, University of Delaware). UDSpace. http://udspace.udel.edu/handle/19716/21493

Wisconsin Department of Transportation. (2021). *Bridge manual*. https://wisconsindot.gov/Pages/Doing-Bus/Eng-Consultants/Cnslt-Rsrces/Strct/Bridge-Manual.Aspx

About the Joint Transportation Research Program (JTRP)

On March 11, 1937, the Indiana Legislature passed an act which authorized the Indiana State Highway Commission to cooperate with and assist Purdue University in developing the best methods of improving and maintaining the highways of the state and the respective counties thereof. That collaborative effort was called the Joint Highway Research Project (JHRP). In 1997 the collaborative venture was renamed as the Joint Transportation Research Program (JTRP) to reflect the state and national efforts to integrate the management and operation of various transportation modes.

The first studies of JHRP were concerned with Test Road No. 1—evaluation of the weathering characteristics of stabilized materials. After World War II, the JHRP program grew substantially and was regularly producing technical reports. Over 1,600 technical reports are now available, published as part of the JHRP and subsequently JTRP collaborative venture between Purdue University and what is now the Indiana Department of Transportation.

Free online access to all reports is provided through a unique collaboration between JTRP and Purdue Libraries. These are available at docs.lib.purdue.edu/jtrp/.

Further information about JTRP and its current research program is available at engineering.purdue.edu/JTRP.

About This Report

An open access version of this publication is available online. See the URL in the citation below.

Wang, Y., Salgado, R., & Prezzi, M. (2026). *Guidelines for use and design of deep foundations for three-sided structures* (Joint Transportation Research Program Publication No. FHWA/IN/JTRP-2026/07). West Lafayette, IN: Purdue University. https://doi.org/10.5703/1288284318615